concentration (10–20 %) of the CGF extract or of serum reduced this gene expression compared with the 0 % control (differentiation medium only) group (Fig. 2). Gene expression of runt-related transcription factor 2 (RUNX2) and of osterix (OSX), the key regulators of osteogenesis, were not significantly changed by treatment with the CGF extract (Fig. 2).

Effect of CGF extracts on proliferation of hTERT-E6/E7 cells

A previous study showed that a first-generation plasma concentrate (Ex.PRP) has a positive dose-dependent effect on cell proliferation [16]. However, other studies have reported the contradictory result that low concentrations of Ex.PRP (a few times greater than physiological levels) are more efficient at enhancing cell proliferation than very high concentrations [17–19]. In this study, the effect of a CGF extract on human mesenchymal stem cell proliferation was assessed by use of a cell count assay and hTERT-E6/E7 cells. In this study, the effect of a CGF extract or serum at concentrations of 1, 3, 5, 10, or 20 % in the culture medium was tested. hTERT-E6/E7 cell proliferation was promoted, in a dose-dependent fashion, by treatment with a CGF extract compared with the effect of serum addition. A significant difference between the effect of CGF and serum on cell proliferation was observed at all concentrations except 20 %. In particular, CGF extract at concentrations of 5 and 10 % markedly increased hTERT-E6/E7 proliferation (Fig. 3a).

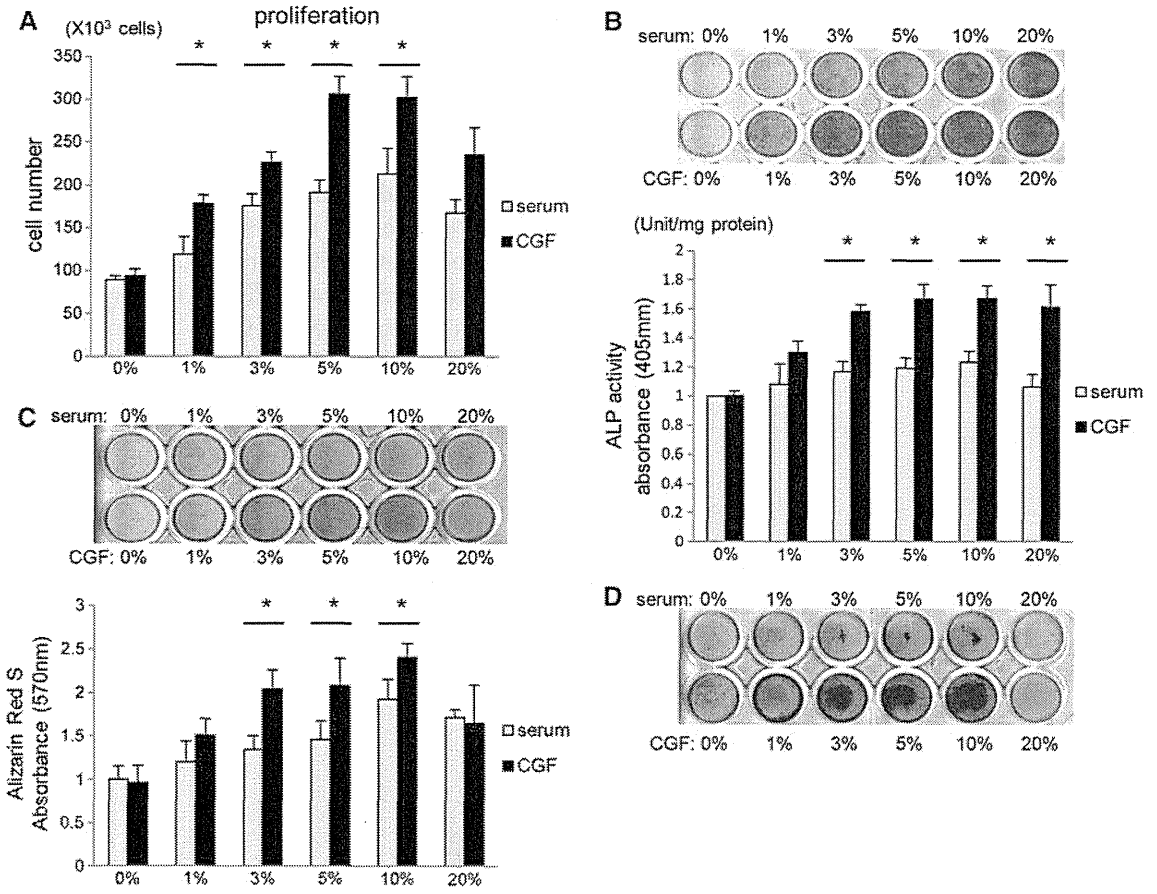

Fig. 3 Effect of a CGF extract on growth and osteoblastic differentiation of hTERT-E6/E7 mesenchymal cells. **a** Cell proliferation. hTERT-E6/E7 cells (5×10^3/well) were treated with different concentrations of a CGF extract or serum control for 24 h after which cell number was counted. **b** Alkaline phosphatase (ALP) staining and enzymatic activity. hTERT-E6/E7 cells were treated with different concentrations of a CGF extract or control serum for 4 days and were then subjected to ALP staining and activity assays. ALP activity was normalized to the protein content of each sample. **c**, **d** Mineralization. hTERT-E6/E7 cells were treated with different concentrations of a CGF extract or control serum for 21 days and were then stained with alizarin red S solution. The Ca content in the matrix of the cells was quantified by measuring the absorbance at 570 nm of the extract of the calcium bound dye. hTERT-E6/E7 cells were treated with different concentrations of a CGF extract or control serum for 21 days and were then stained with von Kossa solution. All data are mean ± SD from three independent experiments (each experiment used CGF from a different volunteer) performed in duplicate. (*$P < 0.05$ compared with the serum group of the same concentration.)

Effect of a CGF extract on the ALP staining and enzymatic activity of hTERT-E6/E7 cells

We next investigated the effect of a CGF extract on osteoblastic differentiation of hTERT-E6/E7 cells by ALP staining and ALP enzyme activity measurement after 4 days treatment with CGF or normal serum. CGF extract treatment increased ALP activity at all concentrations tested compared with the 0 % control (differentiation medium only) group. In addition when compared with equivalent serum dose groups, the CGF-induced increase in ALP activity was significantly different at CGF concentrations of 3–20 % (Fig. 3b).

Effect of CGF extract on mineralization of hTERT-E6/E7 cells

To further confirm the effect of CGF on osteoblastic differentiation, the effect of CGF on the mineralization of hTERT-E6/E7 cells was tested by alizarin red (Fig. 3c) and von Kossa staining (Fig. 3d). hTERT-E6/E7 cells were cultured with differentiation medium containing one of six different doses of a CGF extract or serum for 21 days. Alizarin red and von Kossa staining of these cells showed that CGF at concentrations between 3 and 10 % promoted calcification of the extracellular matrix (ECM) whereas calcification was not clearly observed in cells treated with CGF or serum at a concentration of 20 %. The extent of this ECM calcification was quantified by measurement of the absorbance of the alizarin red S solution. A CGF extract at a concentration between 3 and 10 % significantly increased calcification of the ECM compared with each equivalent concentration of serum.

Typical growth factors and inflammatory cytokines in CGF

We measured typical growth factors and inflammatory cytokines, including PDGF-BB, TGF-β1, TNF-α, and IL-1β, that were secreted by platelets. We found the CGF extract contained these cytokines at concentrations similar to or higher than those in serum. PRP contained high levels of inflammatory cytokines that might inhibit bone formation yet also contained high concentrations of cytokines that might promote bone formation. In a sustained-release test, we found CGF slowly released these cytokines for 9–13 days (Fig. 4).

Treatment of a rat calvaria critical-size bone defect with CGF and BMSCs: Micro-CT analysis

We next investigated the effect of CGF with or without BMSCs on bone regeneration using a representative critical-size bone defect model, the rat calvaria defect model. Representative 3D-reconstructed images of empty defect, CGF, and CGF + BMSC groups, assessed by micro-CT at

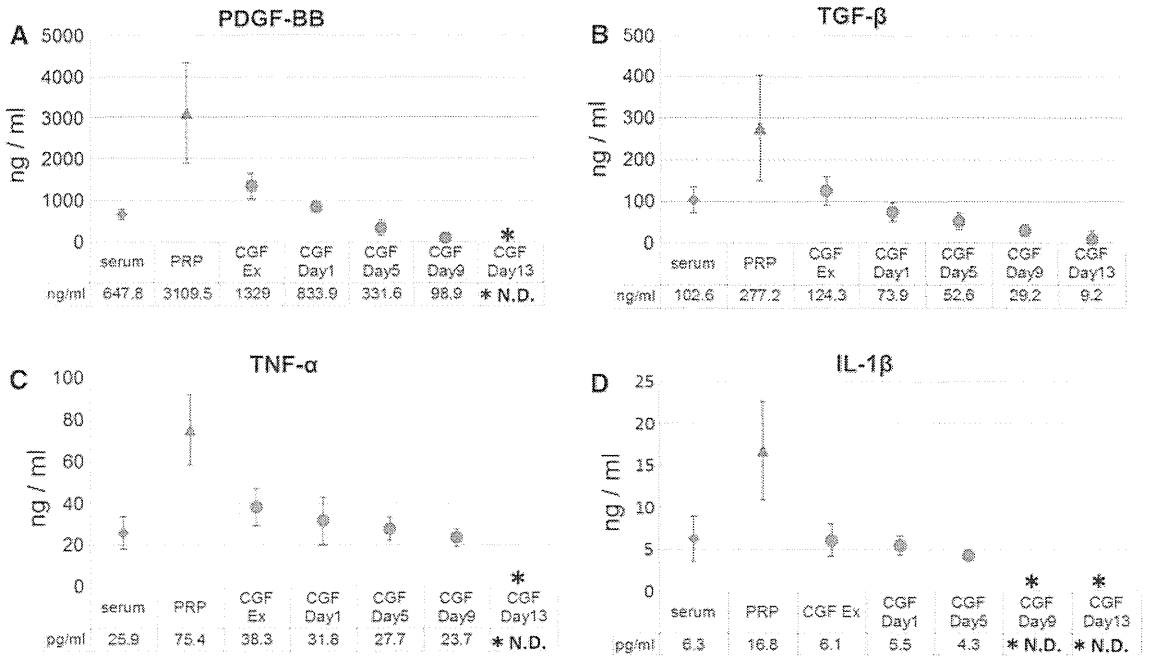

Fig. 4 Measurement of typical platelet cytokines. CGF, PRP, and serum were assayed for PDGF-BB, TGF-β1, TNF-α, and IL-1β by ELISA. In a sustained-release test we incubated CGF for 13 days at 37 °C in centrifuge tubes containing 1,000 μl PBS. The PBS in the tubes was replaced every 2 days and collected for ELISA. CGF slowly released these cytokines. **a** PDGF-BB, **b** TGF-β, **c** TNF-α, **d** IL-1β. *ND* not detected

4, 8, and 12 weeks, are shown in Fig. 5a. An increase in bone formation was observed for all groups over the 12-week period. However, the CGF group and the CGF + BMSC group seemed to regenerate bone better than the control (empty defect) group.

In the control group, bone regeneration was observed only at the periphery of the defect over the 12-week period. In the CGF group, new bone formation started at the peripheral area of the defect and then proceeded toward the center of the defect over time. However, in the CGF + BMSC group, new bone formation was observed not only at the periphery of the bone hole but also in the central area of the defect. This new, central bone included islands of new bone that had no contact with the cut edge of the host bone and that were observed starting from 4 weeks after operation. This group had almost completely repaired critical-size bone defects within 12 weeks after operation.

The total volume of mineralized bone within the defect sites was determined by analysis of the micro-CT images by use of Tri/3D Bon software. As shown in Fig. 5b, the volume of newly formed bone in the CGF + BMSC group was greater than that of the CGF group, and that of the CGF group was greater than that of the control group. Significant differences between the groups were found 4, 8, and 12 weeks after operation except for between the CGF and CGF + BMSC groups at 12 weeks ($n = 6$ for each group/period).

Treatment of a rat calvaria critical-size bone defect with CGF and BMSCs: histological findings

Histological assessment of the osteogenic potential of CGF and CGF + BMSC was performed 4, 8, and 12 weeks after operation in the above-described rat calvaria defect model.

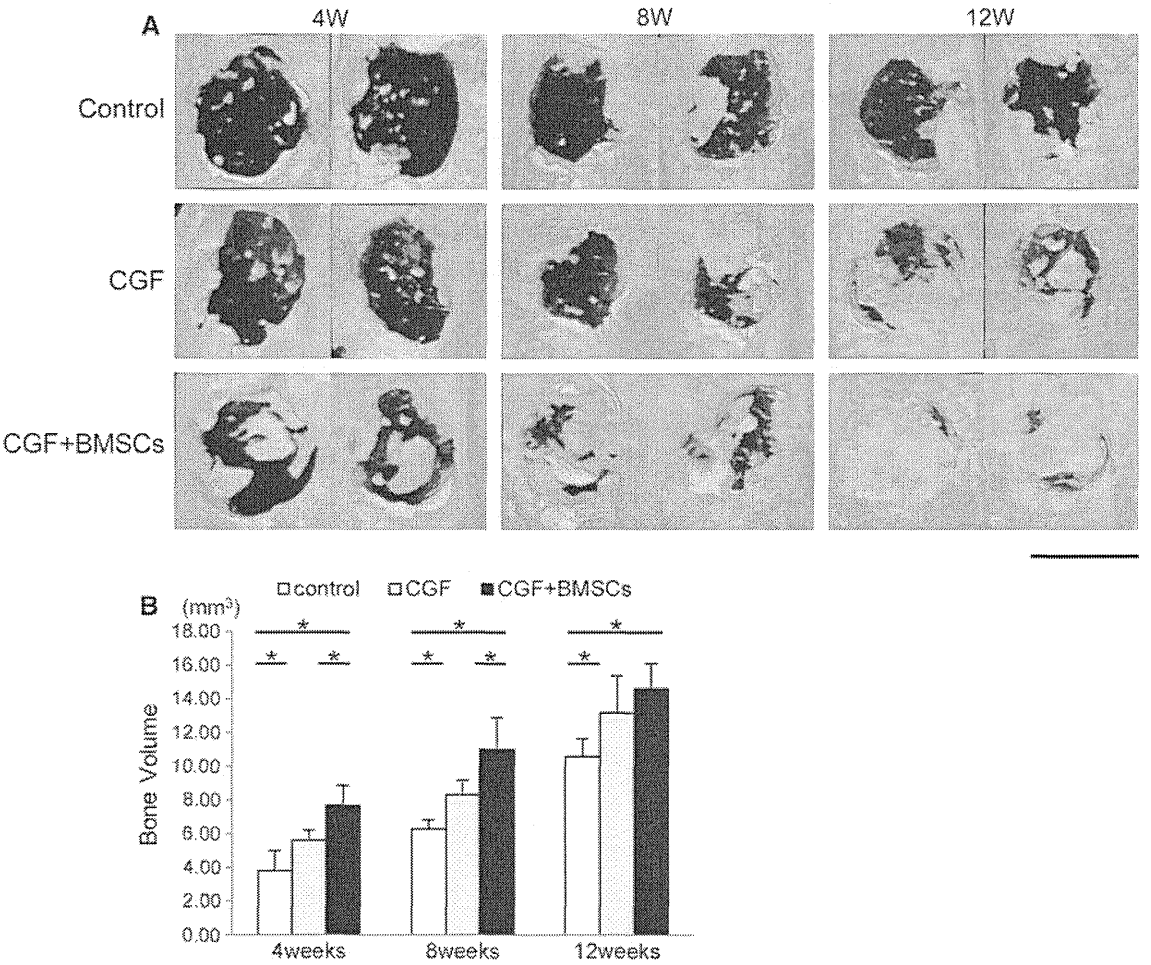

Fig. 5 Treatment of rat calvaria critical-size bone defects with CGF and BMSCs: micro-CT analysis. Bilateral, full thickness, critical-size bone defects (5.0 mm in diameter) were created in the parietal bones of Sprague–Dawley rats. These defects were treated by filling with CGF or CGF + bone marrow stromal cells (BMSCs), or were left unfilled as empty defect controls. **a** Representative microfocus computed tomography (micro-CT) images of cranial samples of the three groups 4, 8, and 12 weeks (W) after operation. *Bar* 5 mm. **b** Calculation of the volume of newly formed bone in calvaria defect sites in the three groups 4, 8, and 12 weeks after operation. All data are mean ± SD from six samples. (*$P < 0.05$)

Hematoxylin and eosin-stained (H&E) sections of bone were examined under a light microscope (Fig. 6a). In addition, we also analyzed 4-week samples by use of polarized light microscopy (Fig. 6b), because calcified immature bone tissue cannot be distinguished from collagenous fibrous tissue on decalcified H&E sections until several weeks after bone formation. Non-calcified woven bone is observed as shiny white fibrous tissue under a polarized light microscope [20, 21].

Histological analysis showed clear differences in tissue formation between the different treatment conditions. In the control group, sparse fibrous connective tissue was observed to traverse the empty defects and newly formed bone was only found in the area adjacent to the edges of the defect site 4 weeks after operation. Woven bone was not clearly observed in polarized microscopic images of the defect site. This pattern of bone formation was also observed after 8 and 12 weeks, except that the new bone at the periphery of the bone hole became thicker over time. Twelve weeks after operation, a large bone defect still remained in the control group.

In the CGF group, similar to the control group, only fibrous connective tissue was observed to traverse the defects and newly formed bone was observed at the edges of the defect site only 4 weeks after operation. However, in contrast with the control group, thin woven bone-like tissue was observed within the defects by polarized light microscopic analysis (Fig. 6b, white arrows). Over time, the new bone at the periphery gradually grew upwards to the central area of the defect site. Twelve weeks after operation, newly formed bone covered a large area of the bone defect.

In the CGF + BMSC group, islands of newly formed bone were observed 4 weeks after operation, which corresponded well with the micro-CT data obtained at this time. In contrast with the other two groups, newly formed bone was found both in the periphery and at the center of the defect site at this time. In addition, abundant neovascularization was observed around the new bone. The new bone became thicker over time, and, 12 weeks after the operation the critical-size bone defect was almost closed and bone marrow was confirmed to be present within the new bone tissues, resulting in a structure similar to that of normal cranial tissues.

Discussion

This study demonstrated that CGF, a second-generation platelet concentrate, effectively promoted the repair of bone defects and had particularly strong effects when combined with BMSCs. In a rat calvarial defect model, combined use of CGF and BMSCs almost completely repaired critical-size bone defects within 12 weeks. In addition, the CGF extract promoted the proliferation, osteogenic maturation, and mineralization of mesenchymal stem cells in vitro.

It is well established that in the rat calvarial defect model there is a gradual progression of new bone from the periphery of the bone hole to the center. New bone progresses in this direction because the cells that induce bone formation are mainly supplied from the cut edge of the bone defect. However, in our study, micro-CT and

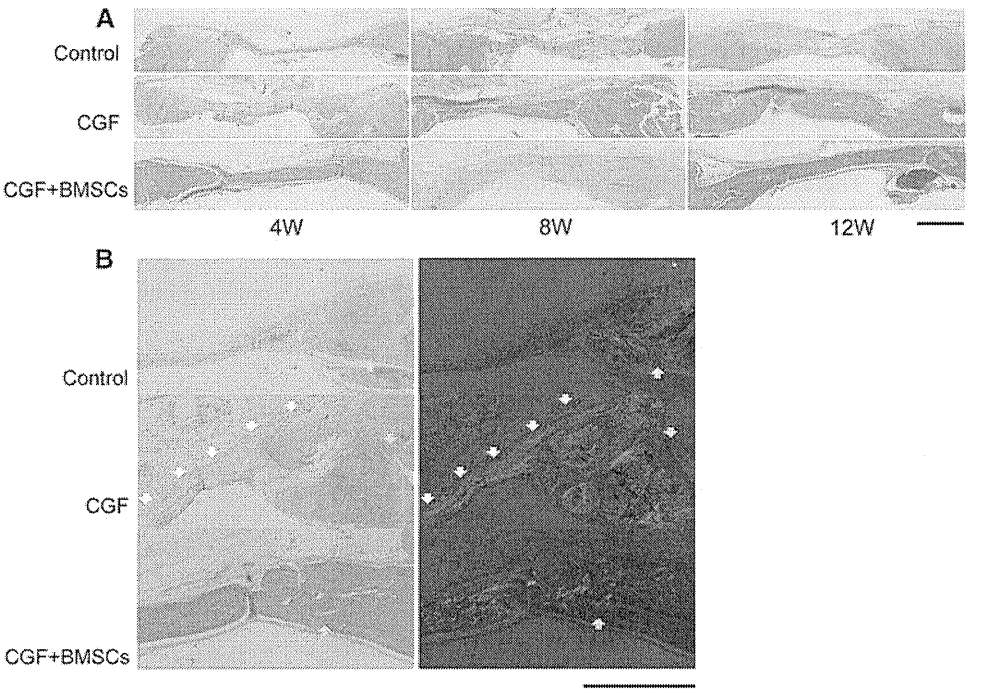

Fig. 6 Treatment of rat calvaria critical-size bone defects with CGF and BMSCs: histological findings. **a** Representative light microscopic images of cranial tissue sections of the three groups, stained with H&E 4, 8, and 12 weeks after operation. (magnification ×20). *Bar* 1,000 μm. **b** Representative light (*left column*) and polarized light (*right column*) microscopic images of H&E stained cranial tissue sections of the three groups 4 weeks after operation, focused on the edges of the cranial holes (magnification ×40). *Bar* 1,000 μm. The *yellow arrows* indicate the edges of the cranial holes. The *white arrows* indicate woven bone tissue (shiny white fibrous tissue)

histological examination revealed new bone formation not only at the periphery of the bone hole but also in the central area of the bone defect in the CGF + BMSCs group, starting 4 weeks after the operation. This new bone included island-shaped new bone that had no contact with the cut edge of the periphery of the bone. Twelve weeks after the operation, critical-size bone defects were almost closed over in the CGF + BMSCs group, whereas large bone defects remained in the control group. This finding suggested that the fibrin network of CGF served as a scaffold for BMSCs that supported the formation of new bone by BMSCs, as reported by Dhohan, Choukroun et al. [2, 22, 23]. In addition, new bone mass significantly increased in the CGF and CGF + BMSCs groups starting 4 weeks after operation, compared with the control group, and this tendency continued until 12 weeks after operation.

Although very favorable results were obtained in these in-vivo experiments, the in-vitro effects of the CGF extract were different depending on the concentration of CGF used. The in-vitro experiments suggested that a highly concentrated CGF extract may inhibit osteogenic maturation and mineralization. Thus, whereas CGF extracts at concentrations between 1 and 10 % promoted cellular proliferation, osteogenic maturation, and mineralization in a dose-dependent manner, the effects of a 20 % CGF extract were inferior to those of the 10 % group, suggesting the existence of optimum doses of CGF. With regard to its effect on *COL1A1* gene expression, expression of this gene decreased in the presence of a high concentration (20 %) of CGF compared with its expression in the control group (0 %), indicating that CGF might actually function to inhibit bone formation. We speculate that this inhibitory effect of CGF might be because, as reported by Dhohan et al. [4], the CGF extract contains not only growth factors favorable for bone formation but also inflammatory cytokines, for example tumor necrosis factor-α (TNF-α) and interleukin-1 (IL-1), which may inhibit bone formation (Fig. 4). Therefore, at a high concentration of CGF the inhibitory action of inflammatory cytokines on bone formation may dominate over the promoting action of the growth factors, which would result in unfavorable effects on bone formation. This concentration-dependent effect seems to be one of the reasons why contradictory effects of PRP on bone formation have been described in previous reports [8–10]. In addition, the results from polymerase chain reaction (PCR) analysis in this study did not reveal any significant change in the expression of such osteogenic master genes as RUNX2 and OSX, which determine whether MSCs are directed toward differentiation into osteoblasts, irrespective of the concentration of CGF extract. These results suggest that the CGF extract stimulates osteogenic maturation only and does not promote commitment of MSCs to osteoblast differentiation.

In this study, we found that CGF served as a good scaffold for BMSCs for treatment of a critical-size bone defect model. The advantages of using CGF as a scaffold are:

1. CGF contains cytokines that promote cell growth, maturation, and matrix production;
2. CGF preparation and cell integration into CGF, are quick and easy; and
3. CGF is safe because it contains nothing but autologous blood ingredients.

For all these reasons we assume CGF will also work as a good scaffold for bone regeneration when it is applied clinically. However, when considering the actual clinical application of combination therapy of CGF and cell transplantation, it will be necessary to optimize the cells to be used (their origin and preparation) and the amount of CGF and other ingredients or modifications that must be applied.

Conclusion

CGF promoted the proliferation, osteogenic maturation, and mineralization of mesenchymal stem cells in vitro, and combination therapy of CGF with BMSCs enabled excellent healing of a critical-size bone defect in vivo. CGF in combination with mesenchymal cell transplantation may be suitable for treatment of large bone defects that are difficult to treat by other methods. However, further research and optimization of the cells and CGF used, and other conditions, are needed before clinical application.

Acknowledgments We thank Dr Junya Toguchida, Kyoto University, for kindly providing the hTERT-E6/E7 cells and Mrs Mari Shinkawa for technical assistance with the histological study. This study was supported by a Grant-in-Aid for Scientific Research (no. 23390364) from the Ministry of Education, Culture, Sports, Science, and Technology, Japan, and by a special research subsidy from Terumo Life Science Foundation. The funders had no role in study design, data collection and analysis, decision to publish, or preparation of the manuscript.

Conflict of interest No competing financial interests exist.

References

1. Mosesson MW, Siebenlist KR, Meh DA. The structure and biological features of fibrinogen and fibrin. Ann N Y Acad Sci. 2001;936:11–30.
2. Dohan DM, Choukroun J, Diss A, Dohan SL, Dohan AJ, Mouhyi J, et al. Platelet-rich fibrin (PRF): a second-generation platelet concentrate. Part I: technological concepts and evolution. Oral Surg Oral Med Oral Pathol Oral Radiol Endod. 2006;101:e37–44.
3. Dohan DM, Choukroun J, Diss A, Dohan SL, Dohan AJ, Mouhyi J, et al. Platelet-rich fibrin (PRF): a second-generation platelet

concentrate. Part II: platelet-related biologic features. Oral Surg Oral Med Oral Pathol Oral Radiol Endod. 2006;101:e45–50.
4. Dohan DM, Choukroun J, Diss A, Dohan SL, Dohan AJ, Mouhyi J, et al. Platelet-rich fibrin (PRF): a second-generation platelet concentrate. Part III: leucocyte activation: a new feature for platelet concentrates? Oral Surg Oral Med Oral Pathol Oral Radiol Endod. 2006;101:e51–5.
5. Brown LF, Lanir N, McDonagh J, Tognazzi K, Dvorak AM, Dvorak HF. Fibroblast migration in fibrin gel matrices. Am J Pathol. 1993;142:273–83.
6. Marx RE, Carlson ER, Eichstaedt RM, Schimmele SR, Strauss JE, Georgeff KR. Platelet-rich plasma: growth factor enhancement for bone grafts. Oral Surg Oral Med Oral Pathol Oral Radiol Endod. 1998;85:638–46.
7. Pietrzak WS, Eppley BL. Platelet rich plasma: biology and new technology. J Craniofacial Surg. 2005;16:1043–54.
8. Plachokova AS, Nikolidakis D, Mulder J, Jansen JA, Creugers NH. Effect of platelet-rich plasma on bone regeneration in dentistry: a systematic review. Clin Oral Implant Res. 2008;19: 539–45.
9. Freymiller EG, Aghaloo TL. Platelet-rich plasma: ready or not? J Oral Maxillofac Surg Off J Am Assoc Oral Maxillofac Surg. 2004;62:484–8.
10. Schmitz JP, Hollinger JO. The biology of platelet-rich plasma. J Oral Maxillofac Surg Off J Am Assoc Oral Maxillofac Surg. 2001;59:1119–21.
11. Dohan Ehrenfest DM, Rasmusson L, Albrektsson T. Classification of platelet concentrates: from pure platelet-rich plasma (P-PRP) to leucocyte- and platelet-rich fibrin (L-PRF). Trends Biotechnol. 2009;27:158–67.
12. Sohn DS, Heo JU, Kwak DH, Kim DE, Kim JM, Moon JW, et al. Bone regeneration in the maxillary sinus using an autologous fibrin-rich block with concentrated growth factors alone. Implant Dent. 2011;20:389–95.
13. Dohan Ehrenfest DM, de Peppo GM, Doglioli P, Sammartino G. Slow release of growth factors and thrombospondin-1 in Choukroun's platelet-rich fibrin (PRF): a gold standard to achieve for all surgical platelet concentrates technologies. Growth Factors (Chur, Switzerland). 2009;27:63–9.
14. He L, Lin Y, Hu X, Zhang Y, Wu H. A comparative study of platelet-rich fibrin (PRF) and platelet-rich plasma (PRP) on the effect of proliferation and differentiation of rat osteoblasts in vitro. Oral Surg Oral Med Oral Pathol Oral Radiol Endod. 2009;108:707–13.
15. Okamoto T, Aoyama T, Nakayama T, Nakamata T, Hosaka T, Nishijo K, et al. Clonal heterogeneity in differentiation potential of immortalized human mesenchymal stem cells. Biochem Biophys Res Commun. 2002;295:354–61.
16. Lucarelli E, Beccheroni A, Donati D, Sangiorgi L, Cenacchi A, Del Vento AM, et al. Platelet-derived growth factors enhance proliferation of human stromal stem cells. Biomaterials. 2003;24:3095–100.
17. Graziani F, Ivanovski S, Cei S, Ducci F, Tonetti M, Gabriele M. The in vitro effect of different PRP concentrations on osteoblasts and fibroblasts. Clin Oral Implant Res. 2006;17:212–9.
18. Weibrich G, Hansen T, Kleis W, Buch R, Hitzler WE. Effect of platelet concentration in platelet-rich plasma on peri-implant bone regeneration. Bone. 2004;34:665–71.
19. Choi BH, Zhu SJ, Kim BY, Huh JY, Lee SH, Jung JH. Effect of platelet-rich plasma (PRP) concentration on the viability and proliferation of alveolar bone cells: an in vitro study. Int J Oral Maxillofac Surg. 2005;34:420–4.
20. Sverzut CE, Lucas MA, Sverzut AT, Trivellato AE, Beloti MM, Rosa AL, et al. Bone repair in mandibular body osteotomy after using 2.0 miniplate system—histological and histometric analysis in dogs. Int J Exp Pathol. 2008;89:91–7.
21. Retamoso LB, Montagner F, Camargo ES, Vitral RW, Tanaka OM. Polarized light microscopic analysis of bone formation after inhibition of cyclooxygenase 1 and 2. Anat Record 2010;293: 195–9.
22. Choukroun J, Diss A, Simonpieri A, Girard MO, Schoeffler C, Dohan SL, et al. Platelet-rich fibrin (PRF): a second-generation platelet concentrate. Part IV: clinical effects on tissue healing. Oral Surg Oral Med Oral Pathol Oral Radiol Endod. 2006; 101:e56–60.
23. Choukroun J, Diss A, Simonpieri A, Girard MO, Schoeffler C, Dohan SL, et al. Platelet-rich fibrin (PRF): a second-generation platelet concentrate. Part V: histologic evaluations of PRF effects on bone allograft maturation in sinus lift. Oral Surg Oral Med Oral Pathol Oral Radiol Endod. 2006;101:299–303.

Original Paper

HORMONE RESEARCH IN PÆDIATRICS

Horm Res Paediatr 2013;79:220–226
DOI: 10.1159/000350520

Received: August 6, 2012
Accepted: March 4, 2013
Published online: May 1, 2013

Detection and Characterization of Two Novel Mutations in the *HNF4A* Gene in Maturity-Onset Diabetes of the Young Type 1 in Two Japanese Families

Makoto Fujiwara[a] Noriyuki Namba[a] Kohji Miura[a] Taichi Kitaoka[a]
Haruhiko Hirai[a] Hiroki Kondou[a] Tsunesuke Shimotsuji[b]
Chikahiko Numakura[c] Keiichi Ozono[a]

[a]Department of Pediatrics, Osaka University Graduate School of Medicine, Suita, [b]Department of Pediatrics, Minoh City Hospital, Minoh, and [c]Department of Pediatrics, Yamagata University School of Medicine, Yamagata, Japan

Key Words
Maturity-onset diabetes of the young · Hepatocyte nuclear factor-4α · *HNF4A* · Mutation · Children

Abstract
Background: Maturity-onset diabetes of the young (MODY) is a subgroup of monogenic diabetes mellitus, of which MODY1, caused by *HNF4A* mutations, accounts for only 5% or less and has been rarely reported in East Asian countries. Here we report two novel *HNF4A* mutations in two Japanese families with MODY1. ***Methods:*** Proband 1 is an 8-year-old girl and proband 2 is a 14-year-old girl. Both were nonobese, demonstrated elevated HbA1c and negative serum anti-glutamic acid decarboxylase antibodies, and had a family history of diabetes. We directly sequenced *HNF4A* and performed functional analysis of the detected missense mutation. ***Results:*** Proband 1 had a heterozygous missense mutation, c.824A>G (p.Asn275Ser). Luciferase assay demonstrated a significant reduction in transcriptional activity. A heterozygous frame shift mutation, c.692–695delAGGA (p.Lys231ThrfsX5), was detected in proband 2. Affected family members shared the same mutations, showing high penetrance. Both mutations reside in the HNF4α dimerization domain and the corresponding amino acids are well conserved between species. ***Conclusions:*** These two mutations are most likely the cause of MODY1 in these families. Considering the effectiveness of sulfonylureas, it is important to correctly diagnose MODY1.

Introduction

Maturity-onset diabetes of the young (MODY) is a monogenic diabetes mellitus (DM) in youth characterized by autosomal dominant inheritance, young age of onset, strong family history, high penetrance and pancreatic β-cell dysfunction. MODY is estimated to be responsible for approximately 2–5% of all cases of DM [1].

At present, heterozygous mutations in at least six different genes have been identified as responsible factors of MODY. These genes encode hepatocyte nuclear factor 4α (HNF4α; MODY1) [2], glucokinase (MODY2) [3, 4], HNF1α (MODY3) [5], insulin promoter factor 1 (MODY4) [6], HNF1β (MODY5) [7] and neurogenic dif-

KARGER

E-Mail karger@karger.com
www.karger.com/hrp

1663–2818/13/0794–0220$38.00/0

Noriyuki Namba, MD, PhD
Department of Pediatrics
Osaka University Graduate School of Medicine
Yamadaoka 2-2, Suita 565-0871 (Japan)
E-Mail nnamba@ped.med.osaka-u.ac.jp

ferentiation factor 1/BETA2 (MODY6) [8]. All the encoded proteins except for glucokinase are transcription factors. MODY2 and MODY3 are the most frequent cause of MODY in all populations studied and they constitute approximately 70% of cases, though the ratio of MODY2 and 3 varies between countries [9]. The other four types of MODY are rare forms.

MODY1 is relatively uncommon among MODY, accounting for less than 5% [9]. The gene responsible, *HNF4A*, encodes HNF4α, a member of the nuclear receptor superfamily of transcription factors. MODY1 is associated with a progressive decrease in insulin secretion, necessitating treatment with oral hypoglycemic drugs or insulin in many cases.

Compared with other types of MODYs, some cases of MODY1 manifest reductions in serum triglycerides, lipoprotein A, apolipoprotein A II and C III [10], and macrosomia or transient neonatal hypoglycemia [11, 12]. In addition, similar to MODY3, MODY1 shows marked sensitivity to sulfonylureas [13] making diagnosis of MODY1 clinically beneficial.

According to a review in 2006, 31 *HNF4A* mutations in 40 families have been identified [14]. However, reports of mutations from East Asian countries including Japan are rare. Only two novel mutations have been reported from Japanese families in the literature [15, 16]. Here, we report two additional *HNF4A* mutations in two Japanese MODY1 families.

Case Report

Family 1

Proband 1 is an 8-year-old Japanese girl who tested positive for glucosuria at a school medical examination. She was born with a birth weight of 4,182 g (+2.8 SD) at a gestational age of 41 weeks and 5 days, without any episodes of asphyxia or hypoglycemia. Her height and weight on initial examination were 135 cm and 32.5 kg, respectively, and her BMI was 17.8. Laboratory tests revealed elevated serum fasting and postprandial glucose, high HbA1c, relatively low apolipoprotein A II, apolipoprotein C III and lipoprotein A, no ketoacidosis, normal serum immunoreactive insulin and C-peptide, negative serum anti-glutamic acid decarboxylase (GAD) and anti-insulinoma-associated tyrosine phosphatase-like protein-2 (IA-2) antibodies, and negative urinary ketones (table 1). Abdominal ultrasonography revealed no abnormalities in the liver, pancreas or kidney. Her father and paternal aunt, who are not obese, were diagnosed as DM in their early thirties and are now being treated with insulin. Her paternal grandfather also suffers from DM (fig. 1a).

The young onset, absence of obesity, noninsulin dependence, negative pancreatic autoantibodies and two generation family history of diabetes suggested the possibility of MODY. Furthermore, due to high postprandial glucose levels, MODY1 or 3, rather than MODY2, was suspected.

Table 1. Clinical summary of probands 1 and 2

	Proband 1	Proband 2
Age at onset, years	8	14
Weight (kg, SDS)	32.5, + 0.8	51.4, + 0.8
Height (cm, SDS)	135, + 0.9	156.8, + 0.9
BMI	17.8	20.9
Weight at birth (g, SDS)	4,182, + 2.8	3,815, + 3.1
HbA1c (NGSP), %	11.5	9.5
Plasma glucose, mg/dl		
Fasting	144	111
2 h after meal or 75 g glucose	394	293
Insulin, μU/ml		
Fasting	4.0	9.87
2 h after meal or 75 g glucose	no data	25.3
Serum C-peptide, ng/ml	1.65	1.73
Total Cholesterol, mg/dl	228	105
Triglyceride, mg/dl	124	179
Apolipoprotein A II, mg/dl[1]	28	ND
Apolipoprotein C III, mg/dl[2]	8.0	ND
Lipoprotein A, mg/dl[3]	12.2	ND
Anti-GAD antibody	negative	negative
Treatment	insulin	glibenclamide and metformin
Complications	none	none

Reference values [10]: [1] Mean ± SE: 37.4±1.6. [2] Mean ± SE: 26.5±2.0. [3] Mean ± SE: 45.2±6.3.

Family 2

Proband 2 is a 14-year-old Japanese girl, who tested positive for glucosuria at a school medical examination. Her birth weight was 3,815 g (+3.1 SD) at a gestational age of 38 weeks and 0 days. She had no hypoglycemic episodes. On presentation, her height and weight was 156.8 cm and 51.4 kg, respectively, and her BMI was 20.9. Laboratory tests revealed high serum fasting blood glucose (126 mg/dl, high HbA1c and negative serum anti-GAD antibody). A 75-gram oral glucose tolerant test demonstrated persistently elevated plasma glucose after 2 h, although a notable amount of residual insulin secretion was detected (table 1). Ophthalmologic evaluation and abdominal ultrasonography revealed no abnormalities. Her mother, maternal grandfather, two maternal great-uncles and maternal great-grandfather had become diabetic in their twenties or thirties (fig. 1b). For the same reason as family 1, MODY1 or MODY3 was suspected.

Materials and Methods

Analysis of the HNF4A Gene

DNA was isolated from peripheral blood leukocytes using the QuickGene DNA whole blood kit S (Fujifilm, Tokyo, Japan) and was amplified by polymerase chain reaction (PCR). *HNF1A* primers were designed using Primer3 (http://frodo.wi.mit.edu/primer3/). Primers for *HNF4A* P1 and P2 promoters [17] and *HNF4A* exons 1–10 [18] were described previously. PCR products were

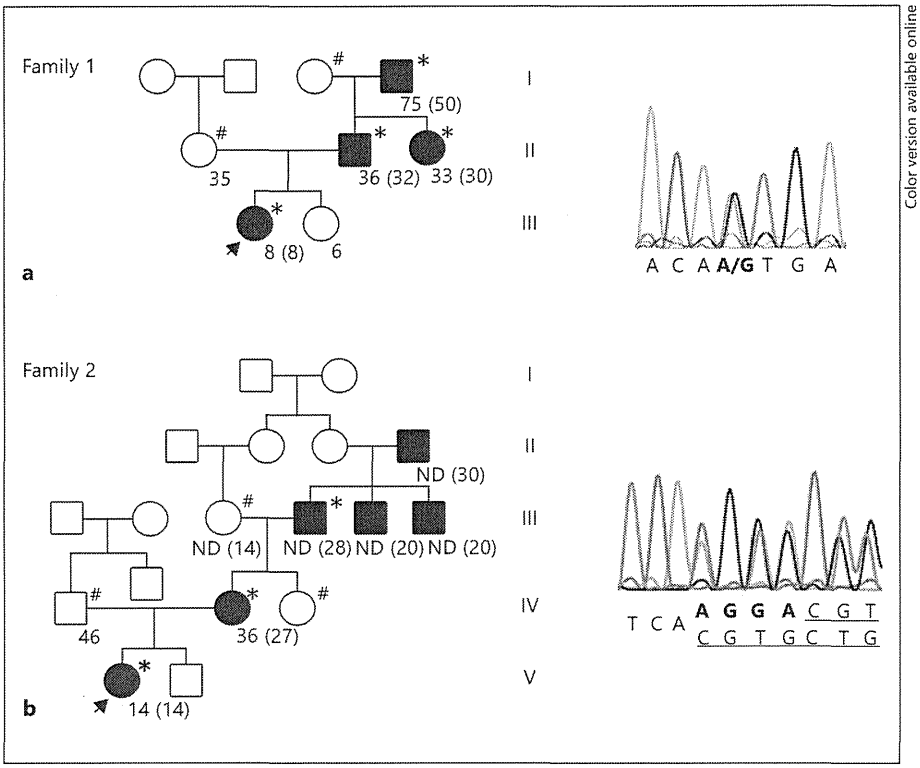

Fig. 1. Pedigrees of the families and the detected *HNF4A* gene mutations. **a** Family 1; missense mutation c.824A>G (p.Asn275-Ser). **b** Family 2; frame shift mutation c. 692–695delAGGA (p.Lys231ThrfsX5). The arrows indicate the probands. The number without parentheses indicates the person's age, and the number with parentheses shows the age of onset. * *HNF4A* mutation positive, # *HNF4A* mutation negative. ND = Not determined.

purified and sequenced using the BigDye Terminator (Applied Biosystems, Foster City, Calif., USA) according to the manufacturer's instructions. The Osaka University Research Ethics Committee approved the study and informed consent for gene analysis was obtained from all participants. The sequence of *HNF1A* is based on GenBank accession number NM_000545.3 (hepatocyte nuclear factor 1-alpha). The sequence of *HNF4A* is based on GenBank accession number NM_000457.3 (hepatocyte nuclear factor 4-alpha isoform b) that corresponds to *HNF4A2*, conventionally used to annotate mutations.

Plasmid Constructs

Full-length, human wild-type *HNF4A8* cDNA was cloned into pcDNA3.1(–) (Invitrogen, Carlsbad, Calif., USA) to create pcDNA3.1(–)/HNF4A vector (HNF4A-WT). We used *HNF4A8* (GenBank accession number NM_175914.4) not *HNF4A2* because the former is driven specifically in pancreatic β cells by the P2 promoter [19]. The mutant pcDNA3.1(–)/HNF4A-Asn275Ser vector (HNF4A-Asn275Ser) was generated by PCR-based mutagenesis using HNF4A-WT as a template and primers containing the nucleotide change. Four luciferase assay reporter constructs using pGVP2 (Toyo Ink) were also prepared. pGVP2-HNF4α2REx3, pGVP2-ApoCIII, pGVP2-ApoAI and pGVP2-HNF1A consisted of three copies of the HNF4α2 response element (5′-GGGTCA-AAGGTCA- 3′) [20], the human apolipoprotein CIII promoter (–1400/+21) [21], the human apolipoprotein AI promoter (–1280 to +220) and the human HNF1A gene promoter (–129/+196) [22], respectively, cloned upstream of the firefly luciferase gene. All vector constructs were verified by bilateral DNA sequencing.

Cell Culture

HeLa cells were maintained in Dulbecco's modified Eagle's medium (DMEM) (Nacalai Tesque, Kyoto, Japan) supplemented with 10% fetal bovine serum (MP Biomedicals, Solon, Ohio, USA) and 1% Insulin-Transferrin-Selenium (Gibco, Carlsbad, Calif., USA) at 37°C with 5% CO_2. HepG2 cells were cultured in DMEM supplemented with 10% fetal bovine serum, 1% nonessential amino acids (Nacalai Tesque) at 37°C with 5% CO_2. MIN6 cells (a gift from Dr. J. Miyazaki, Japan) were cultured in DMEM supplemented with 10% fetal bovine serum, 1% penicillin-streptomycin and β-mercaptoethanol (5 μl/l) at 37°C with 5% CO_2. Upon reaching 80–90% confluence, HeLa cells were detached and plated in 12-well plates at a density of 1×10^5 cells per well. HepG2 and MIN6 cells were plated in 96-well plates at a density of 3×10^4 and 1×10^5 cells per well, respectively. Subsequently, the cells were incubated for 24 h prior to transfection.

Transfection of Wild-Type and Mutant HNF4α

HeLa cells were transfected with a combination of 4 μg HNF4A-WT, HNF4A-Asn275Ser, or empty vector (total up to 8 μg), using FUGENE6 (Roche, Basel, Switzerland) along with 3 μg reporter construct and 0.2 μg phRL-TK (Promega, Madison, Wisc., USA) to control transfection efficiency. For HepG2 cells, lipofectamine 2000 (Invitrogen) was used with 0.4 μg HNF4A-WT, HNF4A-Asn275Ser or empty vector (total up to 0.8 μg), 0.2 μg reporter construct and 0.05 μg phRL-TK, according to the manufacturer's instructions. MIN6 cells were transfected with 1 μg HNF4A-WT, HNF4A-Asn275Ser or empty vector (total up to

2 μg), 0.5 μg reporter construct and 0.05 μg phRL-TK, with the Neon Transfection System (Invitrogen) according to the manufacturer's protocol. Cells were incubated at 37°C with 5% CO_2 for 48 h before harvesting.

Luciferase Reporter Assay

Following a 48-hour incubation, transcriptional activities of wild-type and mutant HNF4α proteins were measured by the Dual-Glo Luciferase Reporter Assay System (Promega). All transfections were carried out in triplicate. We performed six independent experiments.

Western Blot Analysis

All reagents were purchased from Sigma if not indicated otherwise. Forty-eight hours after transfection, HeLa cells in 6-well plates were washed twice with phosphate-buffered saline (PBS) and scraped into 200 μl/well of lysis buffer [150 mM NaCl, 50 mM Tris-HCl (pH 7.5), 1% NP40, 0.25% sodium deoxycholate, 1 mM EDTA with one tablet of protease inhibitor cocktail tablet (Complete Mini, Roche) per 10 ml], sonicated for 2–3 s and centrifuged. The supernatant (5 μg of protein) was fractionated on a 10% sodium dodecyl sulfate-polyacrylamide gel and blotted to a nitrocellulose membrane (TEFCO). The membrane was blocked with PBS containing 5% skimmed milk and then incubated overnight at 4°C with rabbit monoclonal anti-human HNF4α antibody (1:1,000; Cell Signaling Technology, Danvers, Mass., USA). After washing, the membranes were reblocked and incubated for 2 h at room temperature in the presence of horseradish peroxidase-linked donkey anti-rabbit IgG antibody (1:10,000; GE Healthcare, Little Chalfont, UK) and developed using SuperSignal West Dura Extended Duration Substrate (Thermo Scientific, Waltham, Mass., USA). As an internal control, β-actin was detected with a mouse monoclonal anti-β-actin antibody (1:10,000).

Statistical Analysis

Data were expressed as mean ± SD and analyzed with an unpaired t test using JMP software version 8.0.1 (SAS Institute Inc., Carey, N.C., USA). p value <0.01 was considered significant.

Results

Gene Analysis

In proband 1, direct sequencing of the *HNF4* gene revealed a novel heterogeneous missense mutation at nucleotide +824 (c.824A>G) that altered an asparagine to serine (p.Asn275Ser; fig. 1a). This numbering is based on *HNF4A2* and corresponds to c.785A>G, p.Asn262Ser in *HNF4A8*. This variant was not registered in the dbSNP or JSNP databases nor found in 122 alleles of unrelated non-diabetic Japanese controls. Moreover, the asparagine at reside 275 is highly conserved across species (fig. 2). No mutation was found in the *HNF1A* gene. In family 1, identical mutations were detected in the proband's father, paternal aunt and paternal grandfather, but not in the mother or paternal grandmother.

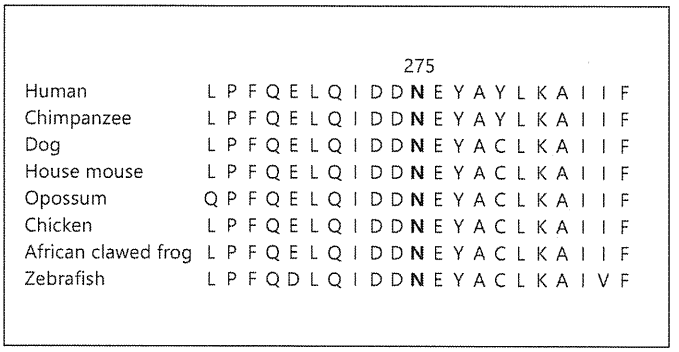

Fig. 2. Alignment of amino acid sequences adjacent to Asn275 from different species. Aligned by ClustalW2 (http://www.ebi.ac.uk/Tools/msa/clustalw2/).

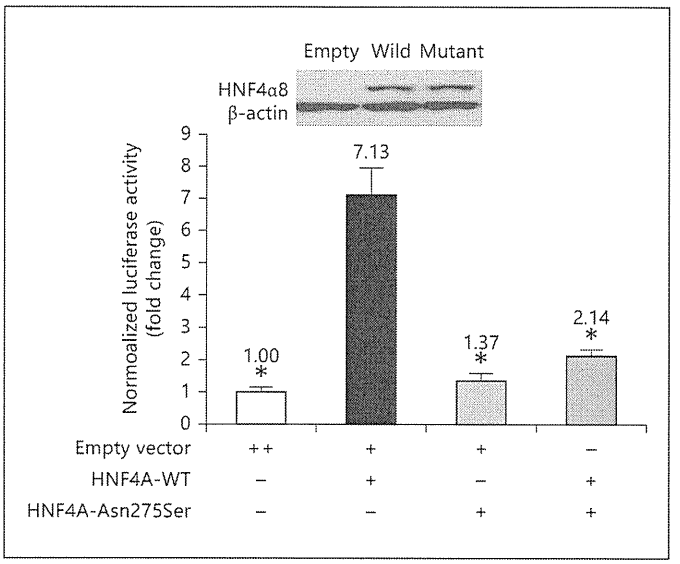

Fig. 3. Transcriptional activity of wild-type and mutant HNF4α in HeLa cells. The inset shows a Western blot demonstrating equal expression of wild-type and mutant HNF4α protein. Error bars indicate ± SD. + = 4 μg plasmid DNA; – = no plasmid DNA. * $p < 0.01$.

In proband 2, analysis of the *HNF4A* gene demonstrated a heterogeneous frame shift mutation in exon 6, c.692–695delAGGA (p.Lys231ThrfsX5; fig. 1b). This numbering is also based on *HNF4A2* and corresponds to c.653–656delAGGA, p.Lys218ThrfsX5 in *HNF4A8*. This mutation was not a known polymorphism. No mutation was identified in the *HNF1A* gene. In family 2, the same mutation was found in the proband's mother and maternal grandfather, while it was not detected in three family members who did not have diabetes.

Functional Analysis

In the experiments carried out in HeLa cells using the reporter construct pGVP2-HNF4α2REx3, the transfection efficiency was more than 90%. Transcriptional activity of HNF4A-Asn275Ser was significantly low, at 19.2% of HNF4A-WT ($p = 0.0003$; fig. 3). The luciferase activity was also significantly lower than HNF4A-WT when HNF4A-Asn275Ser and HNF4A-WT were cotransfected (30.0% of HNF4A-WT, $p = 0.0006$). Western blotting demonstrated equal amounts of wild-type and mutant HNF4α protein expression.

No significant difference in transcriptional activity between HNF4A-WT and HNF4A-Asn275Ser could be shown when using pGVP2-ApoCIII, pGVP2-ApoAI or pGVP2-HNF1A reporter constructs in HeLa cells in our hands (data not shown). In HepG2 or MIN6 cells, the transfection efficiency was low (less than 20%). Experiments using these cells also failed to demonstrate a significant difference.

Discussion

Due to the small number of patients, there has been no systematic review of MODY1 in East Asian countries. The low awareness of MODY1 may cause misdiagnosis as type 1 or 2 DM. Practice guidelines for molecular genetic testing in MODY provided by the Euro Gentest Network of Excellence Project and the European Molecular Genetics Quality Network recommend testing *HNF1A* followed by *HNF4A* for mutations when monogenic DM is suspected and MODY2 has been rejected [9]. According to a recent large analysis of patients suspected of MODY, *HNF4A* mutations were found in 5% of patients who had no *HNF1A* mutations [23]. In this study, we analyzed two families suspected of MODY by clinical features such as young onset, no obesity, noninsulin dependence, negative pancreatic autoantibodies and strong family history. They were diagnosed as MODY1 after ruling out MODY2 based on clinical grounds and MODY3 by gene analysis. We demonstrated *HNF4A* mutations that had not been reported to date in each family.

The *HNF4A* gene encodes HNF4α, a member of the nuclear receptor superfamily of ligand-dependent transcription factors [24]. Two novel mutations were located in exons 6 and 7 that correspond to the dimerization domain of HNF4α. These mutations can potentially affect the ability of HNF4α to form dimers.

In family 1, the p.Asn275Ser mutation showed high penetrance in diabetic family members. A previous report has shown that the p.Glu276Gln is a loss-of-function mutation and this mutation affects DNA binding [25]. In the HNF4α protein, Asn 275 is adjacent to Glu 276, and both are located in helix 8 of the ligand-binding domain, indicating the importance of this location in the transcriptional activity of HNF4α. Transcriptional activity of HNF4A-Asn275Ser was significantly lower than that of HNF4A-WT. Moreover, the dominant negative effect seen in the cotransfection experiment combined with the genetic data strongly suggests that this mutation is diabetogenic. The reporters containing native apolipoprotein CIII, AI or HNF1A promoters demonstrated minimal transcriptional activity in our hands. Though specifically expressed in pancreatic β cells, the transcriptional activity of HNF4α8 is known to be approximately 1–10% of the more commonly used HNF4α2 [26]. This may explain the difficulty in obtaining statistically significant data using these native promoters. The low transfection efficiency in HepG2 and MIN6 cells may also be another reason why we could not obtain statistically significant data in these cells. The fact that Asn 275 is highly conserved between species and that high penetrance was observed in family members makes it highly probable that the p.Asn275Ser mutation is responsible for DM in family 1.

The p.Lys231ThrfsX5 mutation, which also shows high penetrance in affected members of family 2, is a frame shift mutation located in the midportion of the HNF4α protein. Since this mutation truncates the protein, we did not perform functional analysis. From their clinical features, family 2 can be clearly diagnosed as MODY1.

It has been reported that some cases of *HNF4A* mutations are associated with macrosomia and transient neonatal hypoglycemia [11, 12]. Birth weights of both proband 1 and 2 were over +2.5 SD, strongly suggesting the possibility of MODY1. Though still unclear, transient hyperinsulinemia at birth is thought to be the cause of this phenotype. However, both probands did not show hypoglycemia at birth. When a baby born from a non-DM mother presents with macrosomia, the possibility of MODY1 should be considered.

The relatively low levels of serum apolipoprotein A II, apolipoprotein C III and lipoprotein A of proband 1 were also consistent with a previous report [10]. However, another report argues that there is no relationship between these measurements [13]. Furthermore, both probands did not show decreased serum triglyceride levels. There may be genotype-phenotype relationships concerning these parameters in MODY1.

Proband 1 is presently on intensive insulin therapy. Due to poor compliance, hyperglycemia is not well controlled. Since the diagnosis of proband 1 is now confirmed, there is a plan to switch from insulin therapy to sulfonylurea tablets because sulfonylureas are known to be effective for MODY1 [13]. Proband 2 is now well controlled with oral glibenclamide and metformin.

To summarize, two novel *HNF4A* mutations were found in two Japanese MODY1 families. Family 1 demonstrated a heterozygous missense mutation in exon 7. Family 2 showed a heterozygous frame shift mutation in exon 6. Both mutations have high penetrance in the affected members with clinical features of MODY1 and are located in highly conserved lesions. Furthermore, the missense mutation was demonstrated to decrease the transcriptional activity of HNF4α. The nonsense mutation truncated half of the HNF4α protein. Thus, we judged both as responsible for the disease. Making the correct diagnosis allows for improved clinical management (e.g. genetic counseling and planning of treatment possible for the patients). Moreover, considering the effectiveness of sulfonylureas, a definitive diagnosis of MODY1 would be instrumental in maximizing the quality of life of the patients.

Acknowledgments

We thank Prof. J. Miyazaki for generously providing us with the MIN6 cells. We also thank the patients and their families for participating in this study.

References

1 Giuffrida FM, Reis AF: Genetic and clinical characteristics of maturity-onset diabetes of the young. Diabetes Obes Metab 2005;7:318–326.

2 Yamagata K, Furuta H, Oda N, Kaisaki PJ, Menzel S, Cox NJ, Fajans SS, Signorini S, Stoffel M, Bell GI: Mutations in the hepatocyte nuclear factor-4α gene in maturity-onset diabetes of the young (MODY1). Nature 1996; 384:458–460.

3 Froguel P, Vaxillaire M, Sun F, Velho G, Zouali H, Butel MO, Lesage S, Vionnet N, Clément K, Fougerousse F, Tanizawa Y, Weissenbach J, Beckmann S, Lathrop GM, Passa P, Permutt MA, Cohen D: Close linkage of glucokinase locus on chromosome 7p to early-onset non-insulin-dependent diabetes mellitus. Nature 1992;356:162–164.

4 Vionnet N, Stoffel M, Takeda J, Yasuda K, Bell GI, Zouali H, Lesage S, Velho G, Iris F, Passa P, Froguel P, Cohen D: Nonsense mutation in the glucokinase gene causes early-onset non-insulin-dependent diabetes mellitus. Nature 1992;356:721–722.

5 Yamagata K, Oda N, Kaisaki PJ, Menzel S, Furuta H, Vaxillaire M, Southam L, Cox RD, Lathrop GM, Boriraj VV, Chen X, Cox NJ, Oda Y, Yano H, Le Beau MM, Yamada S, Nishigori H, Takeda J, Fajans SS, Hattersley AT, Iwasaki N, Hansen T, Pedersen O, Polonsky KS, Turner RC, Velho G, Chèvre JC, Froguel P, Bell GI: Mutations in the hepatocyte nuclear factor-1alpha gene in maturity-onset diabetes of the young (MODY3). Nature 1996;384:455–458.

6 Stoffers DA, Ferrer J, Clarke WL, Habener JF: Early-onset type-II diabetes mellitus (MODY4) linked to IPF1. Nat Genet 1997;17: 138–139.

7 Horikawa Y, Iwasaki N, Hara M, Furuta H, Hinokio Y, Cockburn BN, Lindner T, Yamagata K, Ogata M, Tomonaga O, Kuroki H, Kasahara T, Iwamoto Y, Bell GI: Mutation in hepatocyte nuclear factor-1β gene (TCF2) associated with MODY. Nat Genet 1997;17:384–385.

8 Malecki MT, Jhala US, Antonellis A, Fields L, Doria A, Orban T, Saad M, Warram JH, Montminy M, Krolewski AS: Mutations in NEUROD1 are associated with the development of type 2 diabetes mellitus. Nat Genet 1999;23:323–328.

9 Ellard S, Bellanné-Chantelot C, Hattersley AT: Best practice guidelines for the molecular genetic diagnosis of maturity-onset diabetes of the young. Diabetologia 2008;51:546–553.

10 Shih DQ, Dansky HM, Fleisher M, Assmann G, Fajans SS, Stoffel M: Genotype/phenotype relationships in HNF-4alpha/MODY1: haploinsufficiency is associated with reduced apolipoprotein (AII), apolipoprotein (CIII), lipoprotein(a), and triglyceride levels. Diabetes 2000;49:832–837.

11 Pearson ER, Boj SF, Steele AM, Barrett T, Stals K, Shield JP, Ellard S, Ferrer J, Hattersley AT: Macrosomia and hyperinsulinaemic hypoglycaemia in patients with heterozygous mutations in the HNF4A gene. PLoS Med 2007; 4:e118.

12 Fajans SS, Bell GI: Macrosomia and neonatal hypoglycaemia in RW pedigree subjects with a mutation (Q268X) in the gene encoding hepatocyte nuclear factor 4α (HNF4A). Diabetologia 2007;50:2600–2601.

13 Pearson ER, Pruhova S, Tack CJ, Johansen A, Castleden HA, Lumb PJ, Wierzbicki AS, Clark PM, Lebl J, Pedersen O, Ellard S, Hansen T, Hattersley AT: Molecular genetics and phenotypic characteristics of MODY caused by hepatocyte nuclear factor 4α mutations in a large European collection. Diabetologia 2005;48: 878–885.

14 Ellard S, Colclough K: Mutations in the genes encoding the transcription factors hepatocyte nuclear factor 1α (HNF1A) and 4α (HNF4A) in maturity-onset diabetes of the young. Hum Mutat 2006;27:854–869.

15 Furuta H, Iwasaki N, Oda N, Hinokio Y, Horikawa Y, Yamagata K, Yano N, Sugahiro J, Ogata M, Ohgawara H, Omori Y, Iwamoto Y, Bell GI: Organization and partial sequence of the hepatocyte nuclear factor-4α/MODY1 gene and identification of a missense mutation, R127W, in a Japanese family with MODY. Diabetes 1997;46:1652–1657.

16 Hara K, Noda M, Waki H, Tobe K, Yamauchi T, Kadowaki H, Satou H, Tsukamoto K, Nagamatsu S, Yamagata K, Matsuzawa Y, Akanuma Y, Kimura S, Kadowaki T: Maturity-onset diabetes of the young resulting from a novel mutation in the HNF-4α gene. Intern Med 2002;41:848–852.

17 Ræder H, Bjørkhaug L, Johansson S, Mangseth K, Sagen JV, Hunting A, Følling I, Johansen O, Bjørgaas M, Paus PN, Søvik O, Molven A, Njølstad PR: A hepatocyte nuclear factor-4α gene (HNF4A) P2 promoter haplotype linked with late-onset diabetes: studies of HNF4A variants in the Norwegian MODY registry. Diabetes 2006; 55:1899–1903.

18 Møller AM, Urhammer SA, Dalgaard LT, Reneland R, Berglund L, Hansen T, Clausen JO, Lithell H, Pedersen O: Studies of the genetic variability of the coding region of the hepatocyte nuclear factor-4α in Caucasians with maturity onset NIDDM. Diabetologia 1997; 40:980–983.

19 Hansen SK, Párrizas M, Jensen ML, Pruhova S, Ek J, Boj SF, Johansen A, Maestro MA, Rivera F, Eiberg H, Andel M, Lebl J, Pedersen O, Ferrer J, Hansen T: Genetic evidence that HNF-1α-dependent transcriptional control of HNF-4 is essential for human pancreatic β cell function. J Clin Invest. 2002;110:827–833.

20 Sladek FM: Hepatocyte nuclear factor (HNF4); in Tronche F, Yaniv M (eds): Liver Gene Expression. Austin, RG Landes., 1994, pp 207–230.

21 Suaud L, Hemimou Y, Formstecher P, Laine B: Functional study of the E276Q mutant hepatocyte nuclear factor-4α found in type 1 maturity-onset diabetes of the young: impaired synergy with chicken ovalbumin upstream promoter transcription factor II on the hepatocyte nuclear factor-1 promoter. Diabetes 1999;48:1162–1157.

22 Yang Q, Yamagata K, Yamamoto K, Cao Y, Miyagawa J, Fukamizu A, Hanafusa T, Matsuzawa Y: R127W-HNF-4α is a loss of function mutation but not a rare polymorphism and causes type II diabetes in a Japanese family with MODY1. Diabetologia 2000;43:520–524.

23 Bellanné-Chantelot C, Lévy DJ, Carette C, Saint-Martin C, Riveline JP, Larger E, Valéro R, Gautier JF, Reznik Y, Sola A, Hartemann A, Laboureau-Soares S, Laloi-Michelin M, Lecomte P, Chaillous L, Dubois-Laforgue D, Timsit J: Clinical characteristics and diagnostic criteria of maturity-onset diabetes of the young (MODY) due to molecular anomalies of the HNF1A Gene. J Clin Endocrinol Metab 2011;96:E1346–E1351.

24 Sladek FM, Zhong WM, Lai E, Darnell JE Jr: Liver-enriched transcription factor HNF-4 is a novel member of the steroid hormone receptor superfamily. Genes Dev 1990;4:2353–2365.

25 Navas MA, Munoz-Elias EJ, Kim J, Shih D, Stoffel M: Functional characterization of the MODY1 gene mutations HNF4(R127W), HNF4(V255M), and HNF4(E276Q). Diabetes 1999;48:1459–1465.

26 Ihara A, Yamagata K, Nammo T, Miura A, Yuan M, Tanaka T, Sladek FM, Matsuzawa Y, Miyagawa J, Shimomura I: Functional characterization of the HNF4α isoform (HNF4α8) expressed in pancreatic β-cells. Biochem Biophys Res Commun 2005;329:984–990.

Circulation Journal
Official Journal of the Japanese Circulation Society
http://www.j-circ.or.jp

ORIGINAL ARTICLE
Pulmonary Circulation

Drastic Shift From Positive to Negative Estrogen Effect on Bone Morphogenetic Protein Signaling in Pulmonary Arterial Endothelial Cells Under Hypoxia

Hiroaki Ichimori, MD; Shigetoyo Kogaki, MD; Kunihiko Takahashi, MD, PhD; Hidekazu Ishida, MD, PhD; Jun Narita, MD; Nobutoshi Nawa, MD; Hiroki Baden, MD; Toshiki Uchikawa, MD; Yoko Okada, MD; Keiichi Ozono, MD, PhD

Background: To investigate the possible role of sex hormones in the pathogenesis of pulmonary arterial hypertension (PAH), the effect of β-estradiol (E2) on bone morphogenetic protein (BMP) signaling, a key signaling pathway involved in PAH, was studied in human pulmonary arterial endothelial cells (HPAEC).

Methods and Results: BMP signaling molecules, including BMP receptor, Smad1/5/8 and Id1, were studied in HPAEC under 1% O_2 (hypoxia) and 21% O_2 (normoxia) as well as the effect of hypoxia-inducible factor (HIF)-1α expression in the presence of E2 on BMP signaling. The effects of an estrogen receptor (ER) antagonist (ICI 182,780) and cycloheximide, and the interaction of ER with Smad or HIF-1α were also studied. In the presence of E2, BMP signaling was augmented under normoxia but suppressed under hypoxia. HIF-1α accumulation suppressed BMP signaling, whereas HIF-1α inhibition augmented signaling. These effects were cancelled by ICI 182,780. Moreover, binding between ER, HIF-1α and phosphorylated (p)-Smad1/5/8 proteins occurred only under hypoxia. On inhibition of de novo synthesis with cycloheximide, however, p-Smad1/5/8 expression was suppressed only under normoxia.

Conclusions: The effects of E2 on BMP signaling in HPAEC altered depending on O_2 concentration and different mechanisms may be involved. BMP and sex hormones may play an important role in PAH development. (*Circ J* 2013; **77:** 2118–2126)

Key Words: Bone morphogenetic protein; Estrogen; Hypoxia-inducible factor

Pulmonary arterial hypertension (PAH) is characterized by pulmonary artery remodeling wherein small peripheral pulmonary arteries are occluded, pulmonary arterial pressure increases, and eventually right heart failure occurs.[1,2] Recent studies have identified the involvement of diverse vascular effectors in the pathogenesis of PAH, such as genetic background, growth factors, and environmental stress. Bone morphogenetic protein receptor (*BMPR*) 1B,[3] activin receptor-like kinase (*ALK*) 1,[4] and *Smad8*[5] mutations as well as *BMPR2* mutation have been reported in idiopathic PAH patients. Because the gene for *BMPR2* was identified as one of those responsible for familial[6,7] and idiopathic[8] PAH, the involvement of BMPR2 in the signal pathway in PAH development has been strenuously investigated. The possibility of PAH development in family members of patients harboring *BMPR2* mutants is only 10–20%, and loss of BMPR2 expression in idiopathic PAH occurs even in the absence of *BMPR2* gene mutations.[9] Therefore, heterozygous *BMPR2* mutations are by themselves insufficient to account for the clinical manifestations of idiopathic PAH, and multiple environmental or genetic "hits" may play a pivotal role in triggering the disease.

Editorial p1992

PAH is estimated to affect 2–3 individuals/million per year, and the incidence of idiopathic PAH in young women is approximately twice that of age-matched men (male:female ratio, 1:2.3). Austin et al reported that the ratio of male to female in 351 PAH patients with BMPR2 mutations was 98:253, showing an overwhelming proportion of female subjects.[10] According to a report by Rosenzweig et al, 23 (16%) of 147 PAH patients had BMPR2 mutations and the male:female ratio was 5:18.[11] Despite much epidemiological evidence, the reason for this female predominance remains unclear. Although estrogen

Received August 2, 2012; revised manuscript received February 27, 2013; accepted March 28, 2013; released online May 18, 2013 Time for primary review: 31 days

Department of Pediatrics, Osaka University Graduate School of Medicine, Suita, Japan
Mailing address: Shigetoyo Kogaki, MD, Department of Pediatrics, Osaka University Graduate School of Medicine, 2-2 Yamadaoka, Suita 565-0871, Japan. E-mail: skogaki@ped.med.osaka-u.ac.jp

ISSN-1346-9843 doi:10.1253/circj.CJ-12-0997

seems to play an important role in the progression of various pulmonary diseases, such as acute lung injury and chronic obstructive pulmonary disease, its role in the pathogenesis and progression of PAH remains controversial.[1,6,12,13]

BMPR2 is a constitutively active serine-threonine kinase that heterodimerizes with and phosphorylates a type I receptor in the presence of a BMP ligand. The activated type I receptor phosphorylates Smad proteins at the C terminus (Smad1, 5, and 8), which then translocate to the nucleus in the presence of a common partner Smad, Smad4, to regulate gene transcription. A major transcriptional target is the inhibitor of the DNA-binding (Id) family of proteins, of which Id1-4 play a central role in the regulation of gene expression, and thus in cellular differentiation and proliferation in response to BMP.[14] In the present study, we refer to the BMPR-Smad1/5/8-Id1 signal pathway as "BMP signaling". Although defective BMP-mediated regulation of cell differentiation and turnover could contribute to abnormal vascular remodeling, the precise mechanism of BMP signaling in this event is unclear.

We previously demonstrated that the expression of BMPR2, phosphorylated (p)-Smad1/5/8, and Id1 was reduced in the lung tissue of hypoxia-exposed Sprague-Dawley rats and hypoxia-exposed rat lung vascular endothelial cells.[15] Both in vivo and in vitro, reduced expression of BMP signaling was predominantly observed in pulmonary arterial endothelial cells (PAEC). Smad1/5/8 and p-Smad1/5/8 expression was also reduced in PAEC of PAH patients.[16] Endothelial dysfunction and proliferation may contribute to PAH and vascular remodeling.[17] Thus, we suggest that hypoxia induces changes in intracellular BMP signaling in PAEC, which are involved in the pathogenesis of PAH, and exposure to hypoxia can mimic the pathogenesis of PAH in vitro. Moreover, reduced expression of BMPR2 has also been found in the lung tissue of monocrotaline-induced pulmonary hypertensive rats.[18] In this study, we focused on hypoxia-inducible factor (HIF)-1α. HIF-1α is an oxygen-dependent transcription factor that regulates the expression of several genes in response to hypoxia. Not only BMPR2 and p-Smad1/5/8 but also HIF-1α is mainly localized in PAEC of PAH patients.[19]

We hypothesized that estrogen and HIF-1α may contribute to PAH development via BMP signaling as components of the multiple epidemiological factors. We found a positive effect of β-estradiol (E2) on BMP signaling in human PAEC (HPAEC) under normoxia and negative effect under hypoxia, and showed that E2-induced de novo synthesized protein is involved in this positive effect, and interaction of the estrogen receptor (ER) with HIF-1α is involved in this negative effect.

Methods

Materials

HPAEC were obtained from Cambrex (Walkersville, MD, USA). Human recombinant BMP2 was purchased from R&D Systems (Minneapolis, MN, USA), E2 and cycloheximide (CHX) from Wako Pure Chemical Industries (Osaka, Japan), ICI 182,780 from Tocris Bioscience (Ellisville, MO, USA) and YC-1 from Chemicon (Billerica, MA, USA). Anti-p-Smad1/5/8 antibody was purchased from Cell Signaling Technology (Beverly, MA, USA), anti-Smad1 antibody from Santa Cruz Biotechnology (Santa Cruz, CA, USA), anti-HIF-1α antibody from Novus Biologicals (Littleton, CO, USA), anti-ERα antibody from Abcam (Cambridge, MA, USA) and anti-β-actin antibody from Sigma Chemical (St. Louis, MO, USA).

Cell Culture

HPAEC were grown in Endothelial basal medium (Cell Applications, San Diego, CA, USA). All experiments were performed using subconfluent cultures of the same batch derived from pooled donors, and were used only between passages 3 and 7. These cells were incubated at 37°C in a humidified atmosphere of 5% CO_2 and air. For exposure to hypoxia, subconfluent cells were placed in an APM-30D incubator (Astec, Fukuoka, Japan) at 37°C in a humidified atmosphere of 1% O_2/5% CO_2/94% N_2. Cells were grown to subconfluence and the medium was changed to phenol-red free serum-starved DMEM. After overnight quiescence, cells were treated for 12 h with 50 ng/ml BMP2 in phenol-red free serum-starved medium with or without E2 under 21% O_2 (normoxia) and 1% O_2 (hypoxia).

Constructs and Luciferase Reporter Assay

The constitutively active HIF-1α expression vector pcDNA3 was kindly provided by Dr Hirota (Kyoto University),[20,21] the −2.1-kb Id1 promoter linked to a luciferase reporter gene (pGL1-Luc) by Dr Katagiri (Saitama Medical University),[22] and the pCMV-estrogen response element (ERE)-luciferase was constructed by Dr Makishima (Nihon University).[23] Transient transfection was carried out using Lipofectamine (Invitrogen, Carlsbad, CA, USA) according to the manufacturer's protocol. The total amount of DNA added to each well was equalized using an empty vector. The luciferase assay was performed in triplicate according to the protocol of the dual luciferase reporter assay system (Promega, Madison, WI, USA). Briefly, 2 days after transfection, cells were cultured with BMP2 and/or E2 and incubated under 1% O_2 (hypoxia) or 21% O_2 (normoxia). Twelve hours later, cells were lysed and luciferase activity was determined using specific substrates in a luminometer. Transfection efficiency was normalized by co-transfection with tK-*Renilla* luciferase construct (Promega).[24]

Western Blot Analysis

Cells were cultured in 60-mm dishes and, after overnight quiescence, were incubated with BMP2 (50 ng/ml) and/or E2 (10^{-7} mol/L) in a phenol red-free serum-free medium for 12 h under 1% or 21% O_2. To prepare whole-cell lysates, cells were washed twice with ice-cold PBS and solubilized in lysis buffer. Lysates were centrifuged at 12,000 *g* for 20 min at 4°C and supernatants were collected. For cell fractionation, cells were washed twice with ice-cold PBS and solubilized in a hypotonic lysis buffer. Lysates were centrifuged at 12,000 *g* for 20 min and supernatants were used as cytosol extracts. The pellet was then lysed with a hypertonic buffer and supernatants were collected after centrifugation (12,000 *g* for 20 min) for use as nuclear extracts. The lysis buffers have been described previously.[24] The protein concentration was determined by the Lowry method using DC reagent (Bio-Rad Laboratories, Hercules, CA, USA). The same amount of sample was separated with sodium dodecylsulfate polyacrylamide gel electrophoresis (SDS-PAGE) and transferred electrophoretically to nitrocellulose membranes. Membranes were blocked in 5% BSA in Tris-buffered saline (TBS). The membranes were then immunoblotted with anti-p-Smad1/5/8 (1:1,000), anti-Smad1 (1:500) or anti-β-actin (1:4,000), and developed with horseradish peroxidase-coupled anti-mouse IgG antibody, followed by enhancement with SuperSignal West Dura Extended Duration Substrate antibodies (Pierce, Rockford, IL, USA). The protein bands were digitally imaged for densitometry using ImageJ (National Institutes of Health, Bethesda, MD, USA).

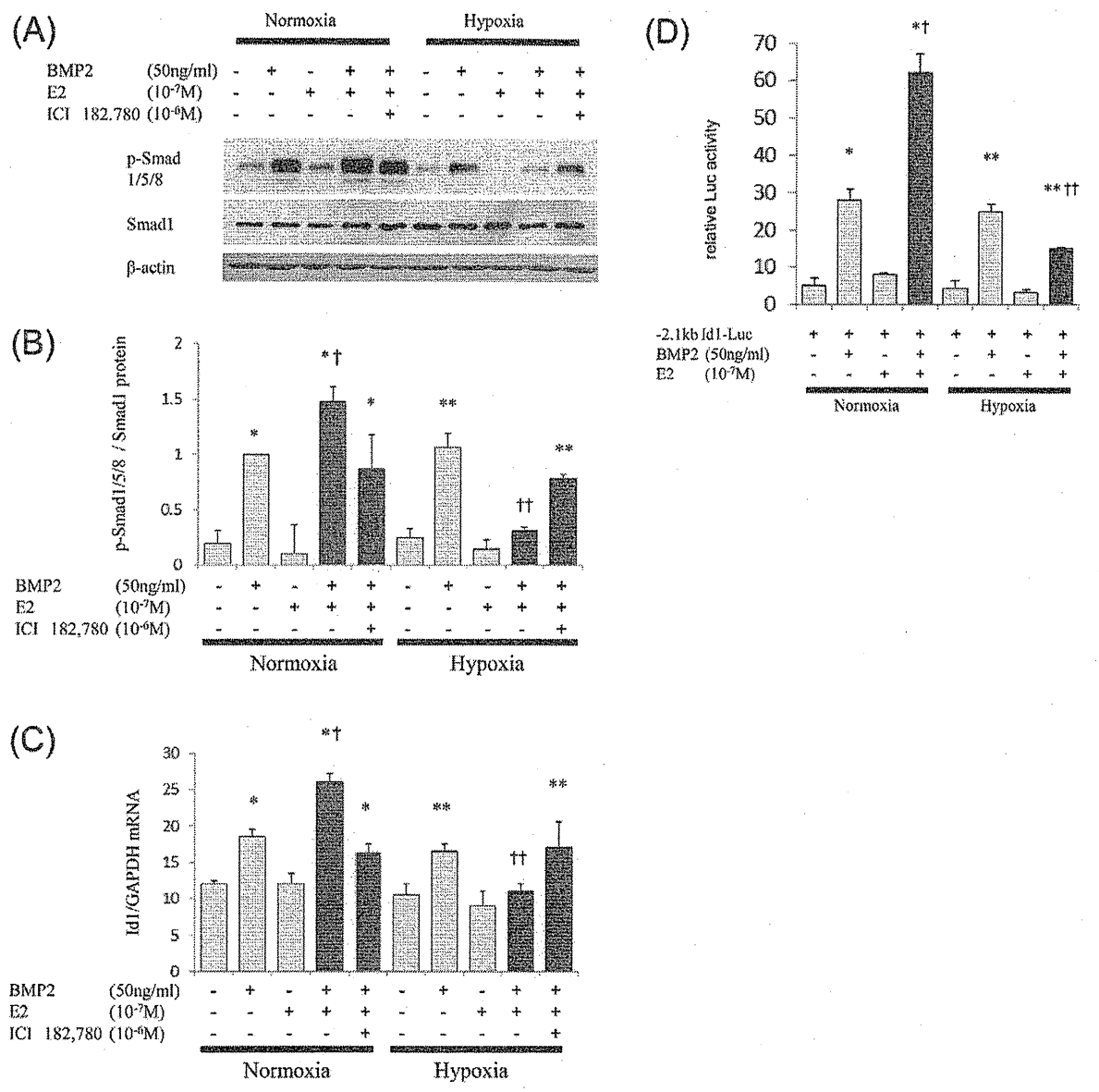

Figure 1. Effects of estrogen on bone morphogenetic protein (BMP) signaling. (**A**) Western blot analysis for p-Smad1/5/8, Smad1 and β-actin proteins. (**B**) Representative expression of p-Smad1/5/8. Relative intensities of the bands were determined by densitometry. Density of p-Smad1/5/8 was normalized against that of Smad1. (**C**) Quantitative RT-PCR analysis of mRNA expression of Id1. Data were normalized by the expression of GAPDH. (**D**) Id1 promoter assay in the presence of BMP2 and/or β-estradiol (E2) under normoxia or hypoxia. Results are presented as the fold induction of luciferase (Luc) activity. Under normoxia, (**A**,**B**) p-Smad1/5/8 proteins, (**C**) Id1 mRNA, and (**D**) Id1 transcriptional activity were significantly increased after the addition of both BMP2 and E2 compared with BMP2 alone, and augmentation of (**A**,**B**) p-Smad1/5/8 proteins and (**C**) Id1 mRNA with BMP2 and E2 treatment was inhibited by the addition of ICI 182,780. Under hypoxia, (**A**,**B**) p-Smad1/5/8 proteins, (**C**) Id1 mRNA, and (**D**) Id1 transcriptional activity were significantly decreased after the addition of both BMP2 and E2 compared with BMP2 alone, and the decrease in (**A**,**B**) p-Smad1/5/8 proteins and (**C**) Id1 mRNA with BMP2 and E2 treatment was recovered by the addition of ICI 182,780. Error bars represent SD. *P<0.05 compared with vehicle under normoxia. **P<0.05 compared with vehicle under hypoxia. †P<0.05 compared with BMP2 alone under normoxia. ††P<0.05 compared with BMP2 alone under hypoxia. Results are representative of at least 3 separate experiments.

Co-Immunoprecipitation Analysis

Lysates were precipitated with anti-ERα or anti-HIF-1α antibody (1:100) at 4°C for 1 h. Protein-antibody complexes were bound to protein G-Sepharose (Sigma) for 1 h, washed extensively with TBS-Tween (0.1%), eluted with buffer as mentioned in Western Blot Analysis, resolved by SDS-PAGE and detected on western blot.

RNA Preparation and Real-Time Reverse Transcription-Polymerase Chain Reaction (RT-PCR)

Total RNA was prepared using the RNeasy Mini Kit (Qiagen, Hilden, Germany) according to the manufacturer's instructions, and reverse transcribed using the High Capacity cDNA Reverse Transcription Kit (Applied Biosystems, Foster City, CA, USA) according to the manufacturer's instructions. Quantita-

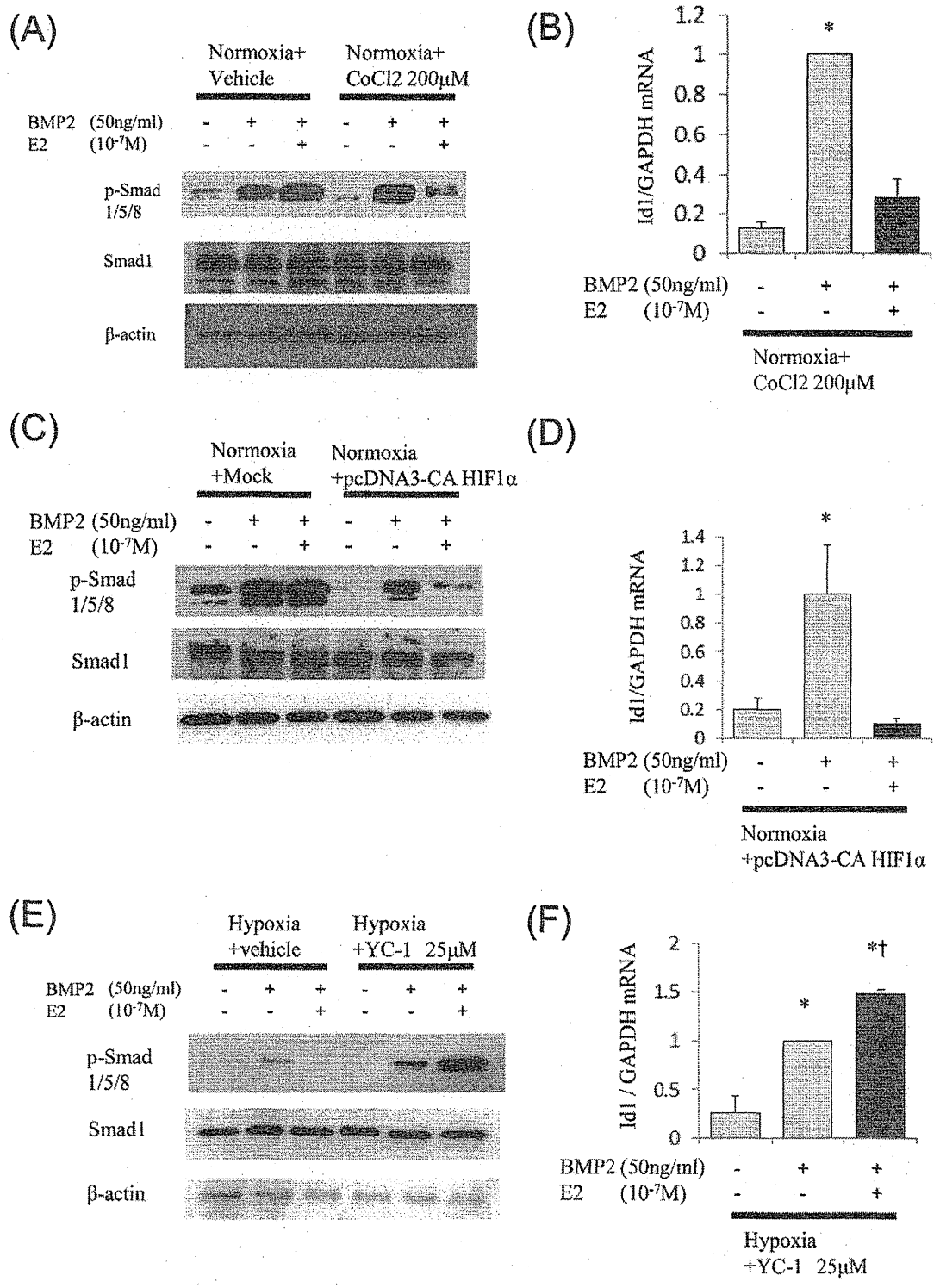

Figure 2. Effect of hypoxia-inducible factor (HIF)-1α regulation. (**A**,**C**,**E**) Western blot analysis for p-Smad1/5/8, Smad1 and β-actin proteins. (**B**,**D**,**F**) Quantitative RT-PCR of Id1 mRNA. Data were normalized by the expression of GAPDH. (**A**,**B**) Under normoxia with CoCl2, (**A**) p-Smad1/5/8 proteins and (**B**) Id1 mRNA were significantly increased with bone morphogenetic protein (BMP) 2 alone compared to vehicle treatment, and the addition of β-estradiol (E2) to BMP2 significantly decreased their expression compared with BMP2 alone. (**C**,**D**) Under normoxia with transfection with constitutively active (CA) HIF-1α plasmid, (**C**) p-Smad1/5/8 proteins and (**D**) Id1 mRNA were significantly increased with BMP2 alone compared to vehicle treatment, and the addition of E2 to BMP2 significantly decreased their expression compared to BMP2 alone. (**E**,**F**) Under hypoxia with YC-1, (**E**) p-Smad1/5/8 proteins and (**F**) Id1 mRNA were significantly increased with BMP2 alone compared to vehicle treatment, and the addition of E2 to BMP2 further enhanced p-Smad1/5/8 protein and Id1 mRNA expression compared to BMP2 alone. *P<0.05 compared with vehicle alone. †P<0.05 compared with BMP2 alone. Results are representative of 3 separate experiments.

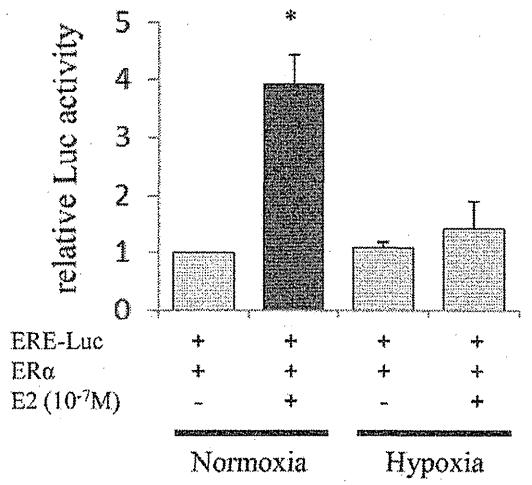

Figure 3. Estrogen transcriptional activity under normoxia and hypoxia. Human pulmonary arterial endothelial cells (HPAEC) were cultured transfected with estrogen response element (ERE)-luciferase. Cells were harvested and relative luciferase (Luc) activity was measured. Results are fold induction of luciferase activity. Estrogen transcriptional activity was significantly increased following treatment with β-estradiol (E2) compared with vehicle treatment under normoxia. *P<0.05 compared with no E2 stimulation under normoxia. Results are representative of 3 separate experiments. ER, estrogen receptor.

tive real-time RT-PCR was performed using TaqMan Gene expression products for human and rat Id1. The *GAPDH* gene was used as an internal standard for quantification (Applied Biosystems).

Pretreatment With CHX

To determine whether E2-induced alteration of p-Smad1/5/8 required de novo protein synthesis, subconfluent HPAEC were treated with CHX (4 μg/ml), an inhibitor of protein translation, 30 min before stimulation with BMP2 and/or E2.

Statistical Analysis

All results are expressed as mean±SD. Statistically significant differences were analyzed on 1-way ANOVA followed by Tukey's multiple comparison post-hoc test. P<0.05 was considered statistically significant.

Results

Effects of Estrogen on BMP Signaling in HPAEC

HPAEC were treated in a serum-free medium with or without E2 in the presence of BMP2 under either normoxia or hypoxia. Cell viability was not affected by estrogen and O_2 concentration in this experiment. We had performed time course experiments at 0.5, 2, 6, 12, and 24 h after use of BMP2 and E2 and found significant changes at 12 and 24 h. We decided to perform all experiments under 12 h incubation. In HPAEC (**Figures 1A,B**), the expression of p-Smad1/5/8 proteins significantly increased following treatment with BMP2 alone compared with vehicle treatment, but no change was observed following use of E2 alone under both normoxia and hypoxia. The amount of p-Smad1/5/8 proteins significantly increased by approximately 60% under normoxia (P=0.026) and decreased by approximately 60% under hypoxia (P=0.040) after the addition of both BMP2 and E2 compared with BMP2 alone.

Similarly, real-time RT-PCR showed that Id1 mRNA expression significantly increased following treatment with BMP2 alone compared with vehicle treatment, and no change was observed in the treatment with E2 alone under both normoxia and hypoxia (**Figure 1C**). Id1 mRNA expression was significantly enhanced under normoxia (P<0.01) and decreased under hypoxia (P<0.01) following the addition of both BMP2 and E2 compared with BMP2 alone.

Effect of ICI 182,780

We confirmed 2 distinct isoforms of ER, ERα and ERβ, in HPAEC on RT-PCR (data not shown). To examine whether the effect of E2 on p-Smad1/5/8 expression was mediated by ER, we added the ER antagonist ICI 182,780 at 10^{-6} mol/L concurrently with E2. Under normoxia, augmented expression of p-Smad1/5/8 proteins with BMP2 and E2 treatment was inhibited by the addition of ICI 182,780. Under hypoxia, decreased expression of p-Smad1/5/8 proteins with BMP2 and E2 treatment was recovered by the addition of ICI 182,780 (**Figures 1A,B**). Similarly, under normoxia, significantly augmented Id1 mRNA expression with BMP2 and E2 treatment was inhibited by the addition of ICI 182,780. Under hypoxia, significantly decreased Id1 mRNA expression with BMP2 and E2 treatment was recovered by the addition of ICI 182,780 (**Figure 1C**). The effects of E2 on p-Smad1/5/8 and Id1 expression were inhibited by ICI 182,780 in HPAEC.

Id1 Promoter Assay

We examined the effects of E2 on transcriptional activity in BMP signaling by performing a –2.1-kb Id1 promoter luciferase assay. In HPAEC (**Figure 1D**), Id1 transcriptional activity significantly increased following BMP2 alone compared with vehicle treatment, and no change was observed following the use of E2 alone under normoxia and hypoxia. Id1 transcriptional activity was increased by approximately 2.6-fold under normoxia (P<0.05) and decreased by 0.5-fold under hypoxia (P<0.05) after the addition of both BMP2 and E2 compared with BMP2 alone.

Effects of HIF-1α Activation

We had examined HIF-1α expression in HPAEC under O_2 concentrations of 1%, 5%, and 21%. HIF-1α expression was observed only in cells cultured under 1% O_2 (data not shown). We examined changes in pSmad1/5/8 and Id1 expression when HIF-1α expression was altered in HPAEC. To modify HIF-1α expression, we used cobalt chloride ($CoCl_2$), plasmids containing constitutively active HIF-1α, or HIF-1α inhibitor (YC-1). When HPAEC were cultured under normoxia with $CoCl_2$ to prevent HIF-1α degradation, the expression of p-Smad1/5/8 proteins and Id1 mRNA was significantly increased with BMP2 alone compared to vehicle treatment, and the addition of E2 to BMP2 decreased their expression compared with BMP2 alone (**Figures 2A,B**). When HPAEC were cultured under normoxia with transient transfection of constitutively active HIF-1α, the expression of p-Smad1/5/8 proteins and Id1 mRNA was significantly increased with BMP2 alone compared to vehicle treatment, and the addition of E2 to BMP2 decreased their expression compared to BMP2 alone (**Figures 2C,D**). In contrast, When HPAEC were cultured under hypoxia with YC-1, the expression of p-Smad1/5/8 proteins and Id1 mRNA was significantly increased with BMP2 alone compared to vehicle treatment, and the addition of E2 to BMP2 further increased p-Smad1/5/8 protein and Id1 mRNA expression compared to BMP2 alone (**Figures 2E,F**).

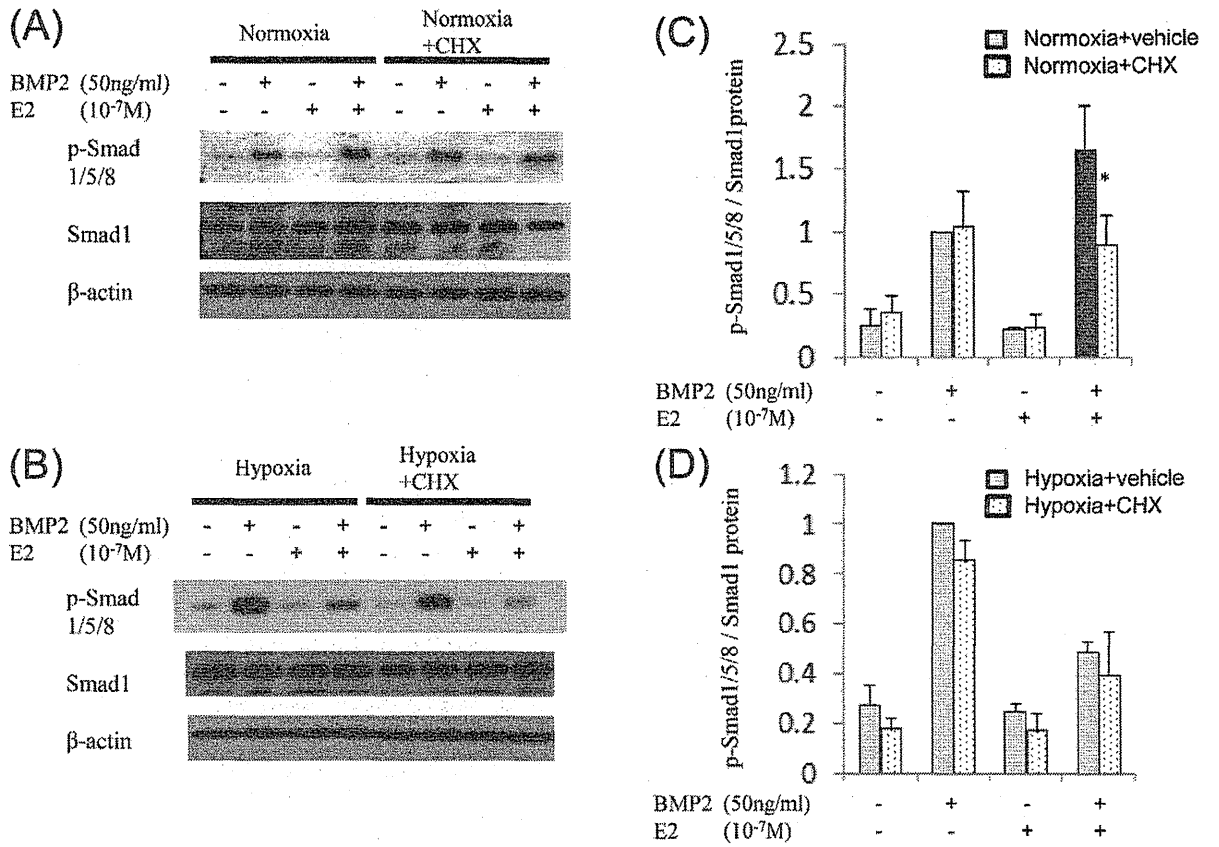

Figure 4. Effect of cycloheximide (CHX) on β-estradiol (E2)-mediated bone morphogenetic protein (BMP) signaling. Human pulmonary arterial endothelial cells (HPAEC) were treated with (black bar) or without (white bar) CHX, an inhibitor of protein translocation, 30 min before stimulation with BMP2 and/ or E2 under normoxia or hypoxia. (**A**,**B**) Western blot analysis of p-Smad1/5/8, Smad1 and β-actin proteins under (**A**) normoxia and (**B**) hypoxia. (**C**) Relative intensities of the bands at (**A**) were determined on densitometry. CHX suppressed the E2-induced augmentation of p-Smad1/5/8 under normoxia. (**D**) Relative intensities of the bands at (**B**) were determined on densitometry. CHX pretreatment had no effect under hypoxia. The density of p-Smad1/5/8 was normalized against that of Smad1. *P<0.05 compared with CHX pretreatment. Results are representative of 3 separate experiments.

ERE Reporter Assay

To investigate whether the transcriptional activity of estrogen in HPAEC was altered under normoxia or hypoxia, we examined the ligand-dependent transcriptional activation of ER by performing an ERE-luciferase assay. The ERE-containing reporter plasmid was transiently transfected into HPAEC. After 12 h of treatment with E2, ERE-mediated transcription was increased by approximately 2.5-fold under normoxia ($P<0.05$), but was not altered by E2 alone under hypoxia (**Figure 3**).

Effect of CHX Pretreatment

To ascertain whether an alteration of p-Smad1/5/8 expression in response to estrogen was required for de novo protein synthesis, HPAEC were subjected to normoxia or hypoxia with or without CHX pretreatment. CHX suppressed the E2-induced augmentation of p-Smad1/5/8 expression under normoxia (**Figures 4A,C**). In contrast, CHX pretreatment had no effect under hypoxia (**Figures 4B,D**).

Interactions Between BMP Signaling, ER, and HIF-1α

To investigate interactions between BMP and E2-ER signaling, we tested the physical interaction between p-Smad1/5/8 and ER and/or HIF-1α in a co-immunoprecipitation experiment. As shown in **Figures 5A,B**, binding was observed among p-Smad1/5/8, ER, and HIF-1α proteins under hypoxia in cells treated with BMP2 and E2, whereas no binding was observed under normoxia. This binding was specifically localized in the nucleus (**Figure 5C**).

Discussion

Recent studies have found that multiple genetic factors are involved in the pathogenesis of PAH. Among them, dysregulated BMP signaling has been thought to play a key role in the onset and development of PAH.[25,26] Here we elucidated the effect of estrogen on BMP signaling in HPAEC: (1) the effect of estrogen on BMP signaling in HPAEC differed depending on the O_2 concentration; (2) the O_2 concentration-dependent changes in BMP signaling produced by E2 are mediated by the level of HIF-1α expression; and (3) entirely different mechanisms are involved in the degradation of HIF-1α expression compared with the augmentation of HIF-1α expression.

First, we showed that the effect of estrogen on BMP signaling in HPAEC differed depending on the O_2 concentration. Under normoxia, the addition of E2 in the presence of BMP2 enhanced BMP signaling in HPAEC, whereas it attenuated

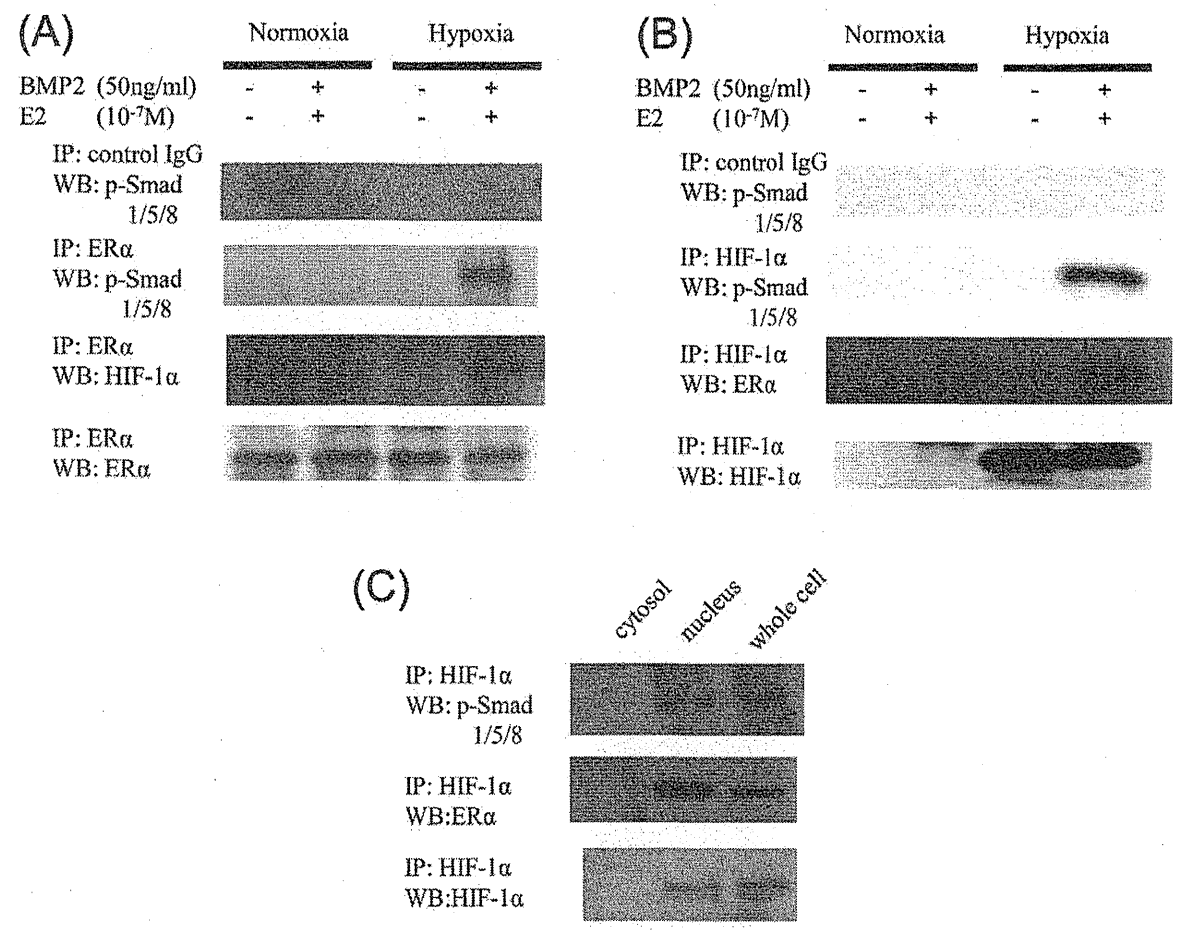

Figure 5. Interactions between p-Smad1/5/8, estrogen receptor (ER) α and hypoxia-inducible factor (HIF)-1α. Human pulmonary arterial endothelial cells (HPAEC) were cultured under normoxia or hypoxia for 24 h, then were either left untreated or treated with bone morphogenetic protein (BMP) 2 and/or β-estradiol (E2) for 12 h. (**A**) Total cell lysates were then immunoprecipitated (IP) with anti-ERα antibody and immunoblotted (WB) with anti-p-Smad1/5/8, anti-HIF-1α or anti-ERα antibody. (**B**) Total cell lysates were IP with anti-HIF-1α antibody and immunoblotted with anti-p-Smad1/5/8, anti-ERα or anti-HIF-1α antibody. Protein-protein binding was observed among p-Smad1/5/8, ER, and HIF-1α (**A**,**B**) under hypoxia treated with BMP2 and E2. (**C**) After treatment with BMP2 and E2 under hypoxia, lysates from cytosol extracts or nuclear extracts were prepared then IP with anti-HIF-1α antibody and immunoblotted with anti-p-Smad1/5/8, anti-ERα or anti-HIF-1α antibody. This binding was specifically localized in the nucleus. Results are representative of 3 separate experiments.

the signaling under hypoxia. These changes were inhibited by treatment with ICI 182,780, an ER antagonist. Thus, E2 acted through ER in these phenomenon. Previously, E2 has been shown to affect BMP signaling in various types of mammalian cell. Yamamoto et al reported that the addition of E2 in the presence of BMP2 suppressed BMP signaling in MCF-7 and HEK293 cells,[27] whereas Paez-Pereda et al reported increases in BMP signaling in GH3 cells after the addition of E2 in the presence of BMP2.[28] These studies also showed that additional treatment with the estrogen antagonist ICI 182,780 inhibited such changes in BMP signaling in vitro, suggesting that E2-induced changes in BMP signaling are mediated by ER. In addition, Helms et al reported the involvement of increased BMP signaling in the progression of ER-positive breast cancer.[29] These observations clearly indicate the presence of cross-talk between BMP and estrogen signaling in various cell types. Here we have shown for the first time that the cross-talk in HPAEC changes its effect depending on O_2 concentration.

Second, we focused on HIF-1α expression in HPAEC because HIF-1α is an important O_2-dependent transcription factor that regulates the expression of several genes in response to hypoxia. HIF-1 is a heterodimeric transcription factor consisting of an inducible α-subunit and a constitutively expressed β-subunit. Previous studies demonstrated that HIF-1α is strongly expressed in PAEC of PAH patients.[19,30] The present study indicated that the O_2 concentration-dependent changes in BMP signaling induced by E2 may be associated with the expression of HIF-1α.

Next, we proposed that entirely different mechanisms were involved under normoxia or hypoxia regarding the changes in BMP signaling induced by E2. Under normoxia, the results of reporter assays using a plasmid containing ERE showed that estrogen transcriptional activity was significantly increased by the addition of E2. In addition, when de novo synthesized proteins were inhibited by CHX under normoxia, E2-augmented phosphorylation of Smad1/5/8 was significantly inhibited. These findings indicate that de novo synthesized proteins produced by E2-ER binding may facilitate BMP signaling under